Czech University of Life Sciences

Faculty of Environmental Sciences

Ecological Engineering – Nature Conservation

Differences in landscape surface temperature within organic and conventional fields - territory of northern and central Bohemia

Diploma Thesis

Author: Bc. Patrik Manda

Thesis supervisor: Ing. Vratislava Janovská PhD.

Prague 2018

CZECH UNIVERSITY OF LIFE SCIENCES PRAGUE

Faculty of Environmental Sciences

DIPLOMA THESIS ASSIGNMENT

Bc. Patrik Manda

Nature Conservation

Thesis title

Differences in landscape surface temperature within organic and conventional fields – territory of northern and central Bohemia

---

Objectives of thesis

The aim of this diploma thesis is to compare the impact of agriculture under organic and conventional management on the local climate within specific area of northern and central Bohemia by remote sensing analysis. For such an analysis is used satellite imagery data from Landsat 8 OLI/TIR spacecraft, ran by United States Geological Survey (USGS) and vector data from Land Parcel Identification System (LPIS) operated by Czech Ministry of Agriculture.

The main research questions are:
Is there any difference in land surface temperature regarding organic and conventional farming management?
Can surface temperature on field hypothetically influence the local climate of the studied site?

Methodology

The author will make quantitative analysis of land surface temperature of organic field in comparison to conventional field in territory of northern and central Bohemia. As input data will be used Landsat 8 imagery and LPIS vector data. It is necessary to calculate thermal images from raw Landsat 8 data, in this case using ArcGIS tool. Results will be pairs of fields (organic and conventional type of management) with almost identical properties (e.g. orientation, area, location, slope, etc.) on which will be possible to compare exact land surface temperatures during a year. For higher validity of the results, whole output will be statistically evaluated. Experiment will be done within 3 years – 2015, 2016 and 2017.

The proposed extent of the thesis

50 – 60 stran

Keywords

access to land, new farmers, land tenure security, agroecology, Terre de Liens, Regionalwert AG, Eco Ruralis

---

Recommended information sources

BAHNER T., DIERMAYR X., SCHMID T., SCHWEDELER A., ZAISER M., ZUCKER I., 2012: Releasing the True Value of Land. International Biodynamic Association. Germany

OXFAM, 2012: 'Our Land, Our Lives'. Time Out on the Global Land Rush. Online: https://www.oxfam.org/sites/www.oxfam.org/files/bn-land-lives-freeze-041012-en_1.pdf

RIOUFOL V., WARTENA S., 2011: Terre de Liens: Removing land from the commodity market and enabling organic and peasant farmers to settle in good conditions. Access to Land for Community Connected Farming: 47 – 63

RIOUFOL V., 2011: Lifting the land barrier: The indispensable step towards developing local, sustainable, civic agriculture in Europe. Provisional paper.

SZOCS A., RODRIGUEZ M., SROVNALOVA A., 2015: Land grabbing in Romania. Fact Finding Mission Report. Eco Ruralis Association. Romania

VOLZ P., 2011: The Regionalwert: Creating Sustainable Regional Structures Through Citizen Participation. Access to Land For Community Connected Farming: 65 – 75

Expected date of thesis defence

2015/16 SS – FES

The Diploma Thesis Supervisor

Ing. Vratislava Janovská, Ph.D.

Supervising department

Department of Land Use and Improvement

Electronic approval: 30. 3. 2016

prof. Ing. Petr Sklenička, CSc.

Head of department

Electronic approval: 31. 3. 2016

prof. RNDr. Vladimír Bejček, CSc.

Dean

Prague on 13. 04. 2016

Declaration

I declare that I have developed and written this Diploma Thesis completely by myself. Any thoughts from others or literal citations are clearly marked and referenced. The research was completed under supervision of Ing. Vratislava Janovská PhD.

Prague, 2018 Patrik Manda

Acknowledgement

Firstly, I would like to thank to my supervisor Ing. Vratislava Janovská PhD. for the useful comments, remarks and engagement through the learning and making process of this thesis. No less, I would like to thank to my great advisor Ing. David Moravec for introducing me to the topic and providing helpful and indispensable advice and consultation on the technical part. Furthermore, I want to thank to my colleague Miroslav Kalenský for helping me with developing the computational script and his critical insight into the problem. Also, I want thank to Ing. Adéla Stanislavová for her constructive criticism while reading the thesis and providing helpful feedback. At the end I would like to express my honest gratitude to my lovely wife Lubi for her borderless and eternal support and comprehension.

Abstract

This thesis focuses on the impact of agriculture on the local climate, namely differences in land surface temperature (LST), regarding two different types of management (organic or conventional), using remote sensing data (Landsat 8 satellite). Based on processing and calculations of the thermal images, which capture the 3-year period (2015, 2016 and 2017) and cover the territory of northern and central Bohemia, the basis for monitoring LST differences between organic and conventional fields has been created. For the following analysis, a computational script has been developed to monitor the trend of these differences and statistically test them. The output from this thesis shows that a certain trend of LST changes between different types of fields actually exists and is even periodically repeated within each tested year. Based on the results, it is relatively likely to say that LST is higher on organic fields in spring and summer (from March to August) and lower in autumn and winter (from September to February) in comparison to conventional ones. LST difference fluctuations at 95% significance are within ± 0,7°C.

Key words

Remote sensing, organic farming, conventional farming, land surface temperature

Abstrakt

Tato práce se zabývá problematikou vlivu zemědělství na lokální klima, konkrétně rozdíly teplot povrchu země při použití různých typů managementu (ekologického nebo konvenčního) a to pomocí dat satelitního snímkování (družice Landsat 8). Na základě zpracování a výpočtů termálních snímků, které zachycují období 3 let (roky 2015, 2016 a 2017) a pokrývají střední a severní část Čech, byl vytvořen podklad pro sledování teplotních změn na povrchu ekologických a konvenčních polí. Pro následnou analýzu byl vyvinut výpočetní skript, pomocí něhož je možné sledovat trend těchto změn a statisticky je testovat. Z výstupu této práce vyplývá, že jistý trend teplotních změn mezi různými typy polí skutečně existuje a dokonce se pravidelně opakuje v rámci každého testovaného roku. Na základě výsledků lze s relativně vysokou pravděpodobností říci, že teplota povrchu země je u ekologických polí v porovnání s těmi konvenčními vyšší v období jara a léta (březen až srpen) a naopak nižší na podzim a v zimě (září až únor). Teplotní fluktuace se na 95% hladině významnosti pohybuje v rozmezí ± 0,7°C.

Klíčová slova

Dálkový průzkum Země, ekologické zemědělství, konvenční zemědělství, teplota zemského povrchu

Table of Contents

Abstract **6**

Key words **6**

Abstrakt **7**

Klíčová slova **7**

1. Introduction **10**

2. Aims **11**

3. Literature review **12**

3.1 Does organic farming provide healthy agricultural landscapes? 12

3.1.1 Alternative approaches towards healthy agricultural landscapes 13

3.1.2 What is the impact of different types of agriculture on climate? 13

3.1.3 How to effectively study land surface? 14

3.2 Capabilities of remote sensing to study land surface 15

3.2.1 Landsat Data Continuity Mission 15

3.2.2 Landsat 8 16

3.2.3 Land Surface Temperature 17

3.2.4 Normalized Difference Vegetation Index 19

3.2.5 Land Surface Emissivity 19

4. Methodology **21**

4.1 Used satellite data 21

4.1.1 Earth Explorer 21

4.1.2 Landsat 8 OLI/TIRS data 22

4.2 Land surface temperature 23

4.2.1 NDVI calculation 23

4.2.2 LSE calculation 24

4.2.3 LST calculation 25

4.3 Land Parcel Identification System 28

4.3.1 Data preparation 28

4.4 Pairing algorithm 33
5. Results 35
5.1 Thermal image processing 35
5.2 Paired parcels and final trend 39
5.3 Statistics 41
6. Discussion 44
7. Conclusion 46
8. References 47
9. Annexes 55
9.1 Parcel Pairing Script 55

1. Introduction

When talking about sustainable food, fodder and bio-fuel production, differences between organic and conventional farming systems and its impact on both, the closest neighborhood and the global ecosystem, is nowadays one of the most discussed topics. Whereas the world´s population is rapidly rising and demand for agricultural products is proportionately growing, it is quite understandable that there is no doubt that these needs have to be ensured in a way that is economically efficient and at the same time has as little negative environmental and social impacts as possible. Therefore, in the last few decades, organic farming has been considered as the best candidate so far. However, it is even more necessary to explore in depth its strengths and similarly its weaknesses in order to make a qualified conclusion.

Land management, where the type of farming also firmly belongs, affects the environment to a large extent. The number of effects that can be observed is countless – starting with the effects on the functioning of the ecosystem, animal migration, aesthetics (and a lot of others) to purely quantitative ones. Among those, secondly named, we can definitely include the Land Surface Temperature (LST). This physical parameter can help to clarify many questions about land surface or indicate various trends in land surface behavior. It is, with no doubt, essential variable for environmental scientists, researchers and specialists for detailed monitoring of landscape processes, like surface energy, water balance and drought assessment.

There are few approaches how to measure LST. Especially, in regional or global scale, the only way how to obtain LST is by remote sensing. Current satellite imagery provides worldwide data of relatively high accuracy and within high repetition frequency. It makes satellite imaging an ideal tool for observing trends changing in time.

In this thesis the author will describe one of the mathematical approaches of retrieving the LST from Landsat 8 spacecraft, as well as will make quantitative analysis of LST differences between similar agricultural fields under organic and conventional management in the territory of northern and central Bohemia, within 3 years (2015 – 2017).

2. Aims

The aim of this thesis is to calculate the land surface temperature (LST) from Landsat 8 OLI/TIRS sensor by particular mathematical approach. Based on these retrieved data the author will make comparative numerical analysis of LST on agricultural fields under organic and conventional management and its possible impact on local climate. Analyzed dataset has been chosen within the period of 3 years (2015, 2016 and 2017) and the territory of central and northern Bohemia that matches the coverage of one particular Landsat 8 image (170 × 183 km). All the results will be statistically tested, in order to receive relevant outcome.

The main outcome will be visualized three-year trend (if there is one) of temperature fluctuation during different seasons and its statistical evaluation.

The main research questions of this thesis are:

- Is there any difference in land surface temperature regarding organic and conventional management?

- How can surface temperature on field hypothetically influence the local climate of the studied site?

3. Literature review

3.1 Does organic farming provide healthy agricultural landscapes?

Agriculture nowadays considerably affects the course of society, landscape and the world's ecosystem (Landis, 2017). This human activity is facing immense challenges – to provide food, fodder, materials and fuel. All of this requires a lot of energy, resources and effort. It is estimated that by the end of 2050, the world´s human population can reach over 10 billion people (Department of Economic and Social Affairs, Population Division, 2017). The way, in which food and energy used to support this increasing population will be produced, is fundamentally essential. In fact, agriculture already "occupies" nearly 40% of the ice-free land surface regarding farming or grazing (Ramankutty et al., 2008; Foley et al., 2011). As high yields are supported, the agricultural intensification through crop monocultures, field magnification and increased chemical and mechanical inputs into soil, negative environmental impacts on soil, water, air and biodiversity have emerged (Firbank et al., 2008; Stoate et al., 2009).

Over the last two centuries, European agriculture has been slowly transforming from ''traditional organic'' farming systems (Tello et al., 2016) based on solar, animal and human energy inputs, usually characterized by production for living and heterogeneous small scale land use, to current industrial ''high-external-input'' (Giampietro et al., 2013) forms of agriculture based mainly on fossil inputs (fuel, artificial fertilizers, biocides) and advanced technologies. This current state of conventional intensive farming is characterized by high specialization and distant supply chains, large scale land use and extensive crop monocultures. Despite the argument of feeding mankind and making great advances in productivity, this approach is obviously not working (Tittonell, 2013) and moreover, the growth of industrial food production has come at a high environmental and social cost (Fraňková and Cattaneo, 2017).

In recent years, as another, no less discussed problem is the land tenure, especially in Central and Eastern Europe (Sklenička et al., 2015). Managing the farmland in a sustainable model is directly affected by relationship between the farmer and the land, both economically and socially (Yami and Snyder, 2016). It seems to be that this issue is in direct connection with farmland ownership fragmentation. Pašakarnis et al. (2013) showed that farmland ownership fragmentation can significantly restrict access to land, or reduce the productivity of agricultural labour (Ženka et al., 2016). A high level of ownership fragmentation is an obstacle for individual farming by owner and

reduces the responsibility felt by tenants (mostly represented by medium or large concerns) for land and landscape (Sklenička et al., 2017). Also thanks to that, land tenure can be considered as one of the main drivers of agricultural landscape changes, fragmentation of ownership structure and soil degradation (Krčílková and Janovská, 2016).

3.1.1 Alternative approaches towards healthy agricultural landscapes

An alternative to a constant productivity increase under high-external input farming system can be considered organic farming. Implementing this system is often accompanied with significantly lower farmland degradation (Sklenička et al., 2015), increased species diversity (Kolářová et al., 2015), creation of more prosperous wild-life habitats (Hole et al., 2005), reduction of the risk of pesticides and nitrates infiltration into the ground and surface water (Tuomisto et al., 2012) and last but not least the reduction of greenhouse gases due to its increased ability to fix carbon in the soil (Gomiero et al., 2011). It is commonly considered that organic farming has positive impact on landscape (Dytrtová et al., 2016).

Agroecology is now being increasingly adopted by small and even larger scale farmers worldwide (Hilmi, 2012). One of the factors driving this trend, as showed Brožová and Beranová (2017), is that organic farms tend to be more profitable and fully competitive with those under conventional management. Other reasons, why organic farming starts to be more present are greater understanding of traditions, enthusiasm and sense of responsibility for healthy landscape, which are more or less common to most farmers (Zagata, 2010).

3.1.2 What is the impact of different types of agriculture on climate?

Despite nearly residual uncertainty, it is commonly accepted that Earth´s climate is changing (Karimi et al., 2018). To effectively face and adapt to ongoing climate change, regarding vital services provided by agriculture, organic farming is adequate choice (Chandra et al., 2017). Organic agricultural technologies provide numerous benefits such as abundant soil organic matter and nitrogen, crop yields increase, reduction of fossil energy inputs, soil erosion decrease and effective soil water conservation – exceptionally beneficial under drought conditions (Pimentel and Burgess, 2013). This is generally the case with regard to the impact of climate change on agriculture. But what

can be said from the opposite point of view? What is the impact of agriculture on climate?

Agricultural production plays highly visible role in the context of climate change. Agriculture itself is a major driver of ongoing climate change, representing source of 10% of all European greenhouse gases (GHG) emissions (EEA, 2017) and about 24% of global GHG emissions (IPCC, 2014). It has been demonstrated by Chiriacò et al. (2017) that organic farming is low-carbon approach with a lower contribution to climate change in terms of GHG emissions per hectare than conventional management.

However, monitoring of GHG emissions is not the only way how to assess the impact of land management on local climate. As quite interesting indicator can be used also land use of monitored site as well (Verburg et al., 2009). El-Zeiny and Effat (2017) in their study showed that land use of specified area has significant impact on land surface temperature and it can directly affect the local climate. It was further demonstrated by López et al. (2016) that differences in land surface temperature (LST) within various land use are even greater with rising altitude. Unfortunately, there is lack of sufficient empirical research on this topic and this diploma thesis would like to participate in filling this gap.

3.1.3 How to effectively study land surface?

When it comes to studying the physical properties and behaviors of earth surface, it is possible to take into account more ways how to achieve it – from studying written documents, maps, printed matters up to modern high-tech approaches such as Geographic Information System (GIS) or remote sensing. While considering the monitoring of technical parameters of earth surface like LST, humidity, land use and many others, especially on medium or large scale, the use of satellite monitoring technique is the only way how to do it (Parastatidis et al., 2017). No other available method can deliver such a huge amount of relevant data on a global scale in relatively high quality and high repetition frequency within few hours or days worldwide (Wulder et al., 2016).

Of course, the absolute accuracy (i.e. resolution) of space-born remote sensed data is still in the order of dozens of meters, which is usually not so suitable for site-specific studies. Nevertheless, for purpose of tracking ongoing dynamic natural and climatic

processes and trends in the atmosphere or on the earth surface, remote sensing wins on full line (Schowengerdt, 2007; Irons et al., 2012; USGS, 2015; Roy et al., 2014; Parastatidis et al., 2017).

3.2 Capabilities of remote sensing to study land surface

"*Remote sensing is defined, for our purposes, as the measurement of object properties on the earth's surface using data acquired from aircraft and satellites. It is therefore an attempt to measure something at a distance, rather than in situ*" (Schowengerdt, 2007).

3.2.1 Landsat Data Continuity Mission

Landsat 8 (*Figure 1*), originally known as the Landsat Data Continuity Mission (LDCM), is the long partnership result of The National Aeronautics and Space Administration (NASA) and U.S. Geological Survey (USGS). It was successfully launched on February 11, 2013 ensuring the continuity of the unparalleled Landsat record since 1972 (Irons et al., 2012). Following 3 months of on-orbit verification of LDCM's capabilities by NASA and LCDM partners, the USGS took over mission operations on May 30, 2013, renamed LDCM to Landsat 8, and opened Landsat 8 data access to users worldwide (USGS, 2015).

Figure 1: *Landsat 8 satellite representation* (http://www.spaceflightinsider.com/organizations/nasa/orbital-atk-awarded-contract-to-extend-landsat-mission/)

3.2.2 Landsat 8

Landsat 8 is a science mission and as for the previous Landsat systems, is ran without any operational mandate (Wulder et al., 2011). In comparison to its predecessor (Landsat 7) it has significantly improved imaging capacity and decreased processing time. More than 700 images per day on average are now being acquired and the newly taken images are available to users world-wide within 8 hours from acquisition (Wulder et al., 2016). It is possible to observe dramatic increase in daily acquisitions when combining both satellites (Landsat 7 and 8), which results into nearly 1200 new images added to Landsat archive every day. From this positive fact come scientific and operational benefits now and in the future. The expanded acquisitions are improving all related applications, especially international studies (Loveland and Irons, 2016).

The Landsat 8 satellite carries onboard two sensors, the Operational Land Imager (OLI) and the Thermal Infrared Sensor (TIRS), which Irons et al. (2012) deeply described in their publication. It collects 11 bands of multispectral imagery with 30 m and 100 m spatial resolution respectively (*Tab. 1*). The OLI and TIRS spectral bands remain broadly comparable to the Landsat 7 Enhanced Thematic Mapper plus (ETM+) bands (Barsi et al., 2014).

Table 1: *Band designation for Landsat 8 satellite* (Barsi et al., 2014)

Bands	Wavelength (micrometers)	Spatial resolution (meters)
Band 1 – coastal aerosol	0.43–0.45	30
Band 2 - blue	0.45–0.51	30
Band 3 - green	0.53–0.59	30
Band 4 - red	0.64–0.67	30
Band 5 - near infrared (NIR)	0.85–0.88	30
Band 6 - SWIR 1	1.57–1.65	30
Band 7 - SWIR 2	2.11–2.29	30
Band 8 - panchromatic	0.50–0.68	15
Band 9 - cirrus	1.36–1.38	30
Band 10 - Thermal Infrared 1	10.60–11.19	100
Band 11 - Thermal Infrared 2	11.50–12.51	100

Geometric and geodetic accuracy is significantly better than previous Landsat missions (which are ~11.4 m when referenced to ground control points, and ~37 m in absolute

geodetic accuracy). Actually, Landsat 8 accuracy mostly overtakes the accuracy of current ground control. Development is in full swing to use Landsat 8 images to upgrade ground control, which should lead to significant improvement of geometric stability of the entire Landsat archive. The updated geometry has among other things great advantages for example in observations of ice movement (Fahnestock et al., 2016), where improved geometry of the 15 m panchromatic band (band 8) in combination with the elimination of bright target saturation allows tracking ice sheet displacements with nearly 1 m precision. This illustrates the very good absolute accuracy of images coming from satellite Landsat 8.

3.2.3 Land Surface Temperature

Land surface temperature (LST) is very important parameter for environmental scientists, researches and specialists and for further studies enables the monitoring of landscape processes (Quattrochi and Luvall, 1999), like surface energy, water balance and drought assessment (Kustas and Anderson, 2009; Karnieli et al., 2010; Chrysoulakis et al., 2013). For better and detailed observation of such similar processes, there exists strong demand for frequently acquired data to get solid LST time series (Hansen et al., 2010). Especially at global and regional scales (Masiello et al., 2015), the satellite remote monitoring of surface is the only way how to study as important parameter as land surface temperature without any doubt is (Weng et al., 2004).

While estimating LST from Landsat datasets, it is possible to use 3 different retrieval methods: split-window algorithm (SW), single-channel algorithm (SC) and direct inversions of the radiative transfer-based equation (Jiménez-Muñoz et al., 2014).

- **Split-Window Algorithm** - the SW technique uses two thermal infra-red sensor (TIRS) bands, typically placed in the atmospheric window between 10 and 12 μm. According to Jimenez-Munoz and Sobrino (2008), the main principle of the technique is that the radiance fading for atmospheric absorption is proportional to the radiance difference of simultaneous measurements at two different wavelengths (band 10 and band 11).

- **Single-Channel Algorithm** – accurate LST determination using SC method requires high-quality atmospheric transmittance/radiance code to correctly

estimate the atmospheric features (Yu et al., 2014). The SC algorithm was revised by Jimenez-Munoz et al. (2009). In SC was proposed practical approach consisted of the approximation of the atmospheric functions versus atmospheric water vapor content from a second-order polynomial fit. SC algorithm can be applied to both of the two TIRS bands.

- **Radiative Transfer Equation-Based Method** – in case of radiative transfer equation-based method, the atmospheric profile is derived from the NCEP (National Centers for Environmental Prediction). It uses on-line atmospheric correction tool – Atmospheric Correction Parameter Calculator (NASA, 2018). Retrieved atmospheric profile is used to imitate atmospheric transmittance, downwelling and upwelling radiance from computer code, called MODTRAN (MODerate resolution atmospheric TRANsmission) model (Barsi et al., 2005; Yu et al., 2014). The LST can be calculated by thermal radiance captured at sensor-level, in synergy with obtained atmospheric parameters (Barsi et al., 2003).

According to study of Yu, Guo and Wu (2014), where they compared SW, SC and radiative transfer equation-based method of Landsat 8 TIRS data (on 41 scenes), resulted that LST retrieval from the radiative transfer equation-based method using band 10 has the highest accuracy with RMSE (Root Mean Square Error) ≤1 K (Kelvin). On the other side, SW algorithm had moderate accuracy and the SC method was even worse – it had the lowest accuracy with all scenes. For those methods, which are using single band generally, LST estimated from band 10 has higher accuracy than band 11.

Precise LST information from Landsat is not easily calculated and it is not directly provided as a standard available product. Many studies suggest methods and algorithms for obtaining LST from Landsat data, but it is still not too easy to implement these approaches. Deeper knowledge of this topic is required (Parastatidis et al., 2017).

Band 11 uncertainty

While the Landsat 8´s TIRS bands were designed to provide direct usage of Split-Window surface temperature retrieval algorithms, it is highly recommended to users to avoid band 11 data in quantitative analysis. On this issue, U.S. Department of Interior (2013) officially says: "*Since the launch of Landsat 8 in 2013, thermal energy from*

outside the normal field of view (stray light) has affected the data collected in TIRS Bands 10 and 11. This varies throughout each scene and depends upon radiance outside the instrument field of view, which users cannot correct in the Landsat Level-1 data product. Band 11 is significantly more contaminated by stray light than Band 10".

3.2.4 Normalized Difference Vegetation Index

Normalized difference vegetation index (NDVI) is very useful indicator to identify long-term variations in vegetation cover and its condition (Fu and Burgher, 2015). NDVI value is derived from red and near-infrared band and naturally fluctuates between -1 and +1, depends on vegetation cover. It is positive (i.e. > 0) for green vegetation, neutral (i.e. between -0.1 and +0.1) within areas of little or no vegetation (e.g. urban areas and bare lands) and negative (i.e. < 0) usually above water surface (Fathizad et al., 2017).

According to Xu et al. (2011), changes in vegetation are causing the main land surface temperature (LST) variations which are affiliated with vegetation density. To find a rational and logical interaction between vegetation and surface temperature indexes, extensive researches have been conducted (Agam et al., 2007; Inamdar et al., 2008; Li et al., 2015). It has been confirmed that such a relationship exists and moreover, it has been finally proven that there is a logical relation between NDVI and LST. In another study, Herb et al., (2008) derived the LST for 3 different areas in the United States with different land use and different land cover classes using heat flux. Furthermore, Jianjun et al., (2005) studied the effects of inadequate land use changes on LST by using the Landsat images. Regarding to their results, the authors pointed out that shifts in land use are a principal factor in LST increase. Higher temperatures were in areas with sparse vegetation and lower temperatures in areas with dense vegetation.

3.2.5 Land Surface Emissivity

Temperature is an important magnitude for many environmental models, e.g. energy and matter exchange between atmosphere and surface, weather prediction or climate change. We can obtain clear picture of this magnitude on local, regional or global scales from thermal data provided by satellites imagery. Its sensors directly measure the radiance emitted by surface – land surface emissivity (Valor and Caselles, 1996).

Emissivity of objects on the surface or surface itself can be obtained in more ways. According to Parastatidis et al. (2017), there are three different sources of emissivity, which are considered to allow more accurate LST estimates for different regions and conditions:

(i) Global emissivity map derived from ASTER (Advanced Spaceborne Thermal Emission and Reflection radiometer) data. It refers to the period 2000–2008 and has 100 m × 100 m spatial resolution (Hulley et al., 2015).

(ii) The MODIS (MODerate resolution Imaging Spectroradiometer), which is daily LST and emissivity product with 1 km × 1 km spatial resolution (Wan, 2014).

(iii) Emissivity based on the vegetation fraction. This fraction is usually estimated from NDVI (Carlson and Ripley, 1997; Parastatidis et al., 2017).

4. Methodology

4.1 Used satellite data

For the needs of this analysis, it was necessary to find the relevant data, namely satellite data that would be of sufficient quality (i.e. would have appropriate sensors of high resolution imaging), needed to calculate the thermal images of earth surface. Landsat 8, established and operated by USGS (United States Geological Survey) since 2013, was used as an appropriate satellite. It is necessary to create an account to obtain Landsat 8 data from USGS server. When account is created, user gets the full access to satellite imagery database, which works on searching engine Earth Explorer (U.S.G.S., 2015).

Regarding chosen Landsat 8 dataset, as the area of interest was determined the area which is covered by particular Landsat image and which mostly covers the territory of northern and central Bohemia.

4.1.1 Earth Explorer

As mentioned above, Earth Explorer is special searching engine for browsing and downloading satellite imagery data from USGS servers. User can search for particular image on basis of *Search Criteria*, *Data Sets*, *Additional Criteria* and *Results*.

- In *Search Criteria* part, there are several options how to allocate the area of interest and date of execution. In case of this study the function *Path/Row* was used, where it is possible to manually determine the position of center of wanted image (path = 191, row = 25; equals to Lat: 50° 17´ 11´´ N, Lon: 15° 15´ 35´´ E; territory of northern and central Bohemia). Execution date was given by *Date Range* parameter (01/01/2015 to 12/31/2017; three years in row).

- Further on is the *Datasets* tab. There was used dataset of Landsat 8 OLI/TIRS (*Landsat → Landsat Collection 1 Level-1 → Landsat 8 OLI/TIRS C1 Level-1*). It is necessary to choose this specific dataset, because it contains thermal band (Band 10).

- Next part of searching process is *Additional Criteria*. There are several parameters to assign. The only important for this work are *Land Cloud Cover*

and *Scene Cloud Cover*. Those are expressing the ratio of cloud cover within image. In both cases *Less than 40%* was chosen to provide good visibility of land surface.

- Last tab is *Results*, where user is able to browse all images, filtered by given parameters. Before downloading the data, it is possible to go through image previews, to see suitability of obtained results. Last action is to add all chosen images to chart and download them.

4.1.2 Landsat 8 OLI/TIRS data

Landsat 8 OLI (Operational Land Imager)/TIRS (Thermal Infrared Sensor) carries, among other units, thermal infrared radiometer and therefore its data are suitable for LST estimation (Parastatidis et al., 2017). It contains 11 spectral bands in *TIFF* format (*Tab. 1*), pre-collection quality assessment band also in *TIFF* format, angle coefficients file and metadata file, both in *TXT* format.

- **Spectral bands files** – images consist of nine spectral bands with a spatial resolution of 30 meters for Bands 1 to 7 and 9. The ultra-blue Band 1 is useful for coastal and aerosol studies. Band 9 is useful for cirrus cloud detection. The resolution for Band 8 (panchromatic) is 15 meters. Thermal bands 10 and 11 are useful in providing more accurate surface temperatures and are collected at 100 meters, but are resampled to 30 meter resolution in delivered data product. The approximate scene size is 170 km north-south by 183 km east-west (Barsi et al., 2014).

- **Quality band file** - Pre-Collection Quality Assessment band is an important addition to Landsat 8 data files. Each pixel in the QA band contains integers that represent bit-packed combinations of surface, atmosphere, and sensor conditions that can affect the overall usefulness of a given pixel (U.S.G.S., 2013).

- **Angle Coefficient file** - provides sensor viewing angle model coefficients that can be used to create angle bands, and allows users to compute the solar and sensor viewing angles on a per-pixel basis. Angle bands allow users to better understand how the sensor viewing geometry and solar illumination geometry

affects the object being sensed by the imaging instrument. Angle bands can be utilized in science algorithms to produce more accurate results over the current practice of using a single solar illumination value and sensor viewing angle based on the scene center (U.S.G.S., 2017).

- **Metadata file** - Landsat Metadata files contain beneficial information for the systematic searching and archiving practices of data, and also explain the essential characteristics of the Level-1 data products. Metadata describe individual parameters used during processing of the data, including the processing levels of each scene. Values important for enhancing Landsat data (such as conversion to reflectance and radiance, date of acquisition, scene center coordinates, etc.) are also included in this file (U.S.G.S., 2017).

4.2 Land surface temperature

LST estimation is quite complex process, which is supported by several calculations, software and on-line tools. In this study, in order to retrieve the LST data, was essential to derive these variables: normalized difference vegetation index (NDVI), land surface emissivity (LSE) and finally LST itself. As software tool, used for achieving these objectives, was chosen *ArcGIS 10.4* and *Atmospheric Correction Parameter Calculator* as an on-line tool for calculating atmospheric corrections above the scene.

4.2.1 NDVI calculation

NDVI calculation was done in *ArcGIS* software. However, before calculation itself, it was necessary to do couple of preparative steps.

First, add 4 spectral bands: band 2 (blue light), band 3 (green light), band 4 (red light) and band 5 (near-infrared light). Then those 4 bands were combined by *Composite Bands* tool (*Geoprocessing → ArcToolbox → Data Management Tools → Raster → Raster Processing → Composite Bands*).

After previous steps, NDVI calculation could be made. In *ArcGIS* is special tool, dedicated to this purpose – *NDVI* tool (*Windows → Image Analysis → Processing →*

NDVI), which was used. Vegetation index is generated according to following equation (*Eq. 1*):

$$NDVI = \frac{NIR - RED}{NIR + RED} \quad \text{Eq. (1)}$$

where *NDVI* is normalized difference vegetation index; *NIR* is near infra-red band; and *RED* is red band.

4.2.2 LSE calculation

Emissivity of land surface (LSE) is essential to retrieve LST. For obtaining this variable it is necessary to achieve few steps before. All the calculations were accomplished using *ArcGIS Raster Calculator* tool (*Geoprocessing → ArcToolbox → Spatial Analyst Tools → Map Algebra → Raster Calculator*).

At the beginning it is important to obtain Top-of-Atmosphere (TOA) radiance. OLI and TIRS band data can be converted to TOA spectral radiance using the radiance rescaling factors provided in metadata file of every single image. It was done by formula (*Eq. 2*)222, which is given by U.S. Department of Interior, (2013):

$$L_{TOA} = M_L \cdot Q_{cal} + A_L \quad \text{Eq. (2)}$$

where L_{TOA} is TOA spectral radiance $\left(\frac{Watts}{m^2 \cdot srad \cdot \mu m}\right)$; M_L is band-specific multiplicative rescaling factor from the metadata file (*RADIANCE_MULT_BAND_10 = 0.0003342*); A_L is band-specific additive rescaling factor from the metadata file (*RADIANCE_ADD_BAND_10 = 0.1*); and Q_{cal} is quantized and calibrated standard product pixel values (*digital number of NDVI product*).

After calculating the TOA spectral radiance, it is possible to proceed with retrieval of another important variable, which is proportion of vegetation cover (Sobrino et al., 2004). This element was calculated by following equation (*Eq. 3*):

$$P_V = \left(\frac{NDVI - NDVI_{min}}{NDVI_{max} - NDVI_{min}}\right)^2 \quad \text{Eq. (3)}$$

where P_V is proportion of vegetation cover; *NDVI* is normalized difference vegetation index (*NDVI product*); $NDVI_{min}$ is minimum value of NDVI within the scene (*usually value of 0.2*); and $NDVI_{max}$ is maximum value of NDVI within the scene (*usually value of 0.5*).

As the final step to get LSE is to use the formula (*Eq. 4*) proposed by Sobrino et al., (2004):

$$\varepsilon = 0.004 \cdot P_V + 0.986 \quad \text{Eq. (4)}$$

where ε is land surface emissivity (*unitless*); P_V is proportion of vegetation cover; 0.004 and 0.986 are constants given by Sobrino et al., (2004).

4.2.3 LST calculation

Land surface temperature (LST) is critically important for agricultural field temperature comparison. To meet this goal correctly and with as much accurate absolute results as possible, it is essential to deal with the influence of the atmosphere. The most stable and reliable method is calculating the LST with use of web-based atmospheric correction tool *Atmospheric Correction Parameter Calculator* (ACPC), validated by Barsi et al. (2005).

ACPC is designed on the on-line basis. It operates with NCEP atmospheric profile layers in-situ to about 16 km high, but MODTRAN considers atmosphere end to be at 100 km height. To approximate the highest layers of the atmosphere, a "standard" atmospheric profile is used. The ACPC has two standard atmospheric profiles available: *mid-latitude summer* and *mid-latitude winter* (NASA, 2018). For this study was chosen *mid-latitude summer* for warmer part of a year (scenes acquired from beginning of April till the end of September) and *mid-latitude winter* for colder part of a year (scenes acquired from beginning of October till the end of March).

The other parameters that needed to be filled were: *Year* (stored in metadata; DATE_ACQUIRED), *Month* (stored in metadata file; DATE_ACQUIRED), *Day* (stored in metadata file; DATE_ACQUIRED), *GMT Hour* (stored in metadata file; SCENE_CENTER_TIME), *Minute* (stored in metadata file; SCENE_CENTER_TIME), *Latitude* (for studied scene: +50.2864), *Longitude* (for studied scene: +15.2598), *Use interpolated atmospheric profile for given lat/long, Use Landsat-8 TIRS Band 10 spectral response curve* and e-mail address, where results should be sent. The optional part of ACPC interface was left empty. The resulting output from ACPS are those important variables: upwelling (atmospheric) path radiance, downwelling (sky) radiance and atmospheric transmission.

Based on calculations of Barsi et al. (2005), with appropriate knowledge of the atmosphere and once these parameters are known, it was possible to convert the space-reaching radiance to a surface leaving radiance (*Eq. 5*):

$$L_{TOA} = \tau \cdot \varepsilon \cdot L_T + L_u + \tau \cdot (1 - \varepsilon) \cdot L_d \qquad \text{Eq. (5)}$$

where L_{TOA} is TOA spectral radiance measured by the instrument $\left(\frac{Watts}{m^2 \cdot srad \cdot \mu m}\right)$; τ is the atmospheric transmission (*ACPC output; unitless*); ε is land surface emissivity (*unitless*); L_T is the radiance of blackbody target of kinetic temperature T $\left(\frac{Watts}{m^2 \cdot srad \cdot \mu m}\right)$; L_u is the upwelling or atmospheric path radiance $\left(\frac{Watts}{m^2 \cdot srad \cdot \mu m}\right)$; and L_d is the downwelling or sky path radiance $\left(\frac{Watts}{m^2 \cdot srad \cdot \mu m}\right)$.

It is obvious that this formula (*Eq. 5*) is not sufficient, because the L_T value is missing. For that reason was used modified equation (*Eg. 6*), derived by (Srivastava et al., 2009):

$$L_\lambda = \frac{L_{TOA} - L_u - \tau \cdot (1 - \varepsilon) \cdot L_d}{\tau \cdot \varepsilon} \qquad \text{Eq. (6)}$$

where L_λ is land surface spectral radiance $\left(\frac{Watts}{m^2 \cdot srad \cdot \mu m}\right)$; L_{TOA} is TOA spectral radiance measured by the instrument $\left(\frac{Watts}{m^2 \cdot srad \cdot \mu m}\right)$; τ is the atmospheric transmission (*ACPC output; unitless*); ε is land surface emissivity (*unitless*); L_u is the upwelling or atmospheric path radiance $\left(\frac{Watts}{m^2 \cdot srad \cdot \mu m}\right)$; and L_d is the downwelling or sky path radiance $\left(\frac{Watts}{m^2 \cdot srad \cdot \mu m}\right)$.

Last approach to obtain LST is to convert land surface radiance to temperature. It was made by using the Landsat specific estimate of the Planck curve (*Eq. 7*), derived from Planck equation (Barsi et al., 2005):

$$T_K = \frac{k_2}{ln\left(\frac{k_1}{L_\lambda} + 1\right)} \qquad \text{Eq. (7)}$$

where T_K is the LST in Kelvin; L_λ is land surface spectral radiance $\left(\frac{Watts}{m^2 \cdot srad \cdot \mu m}\right)$; k_1 is the calibration constant from the metadata file (*K1_CONSTANT_BAND_10 = 774.8853*); and k_2 is the calibration constant from the metadata file (*K2_CONSTANT_BAND_10 = 1321.0789*).

For needs of this study was made optional Kelvin to Celsius temperature conversion (*Eq. 8*):

$$T_C = T_K - 273.15 \qquad \text{Eq. (8)}$$

where T_C is the temperature in Celsius; T_K is the temperature in Kelvin; - 273.15 is the Kelvin-Celsius shift constant.

4.3 Land Parcel Identification System

As a reference data frame for calculated data were used Land Parcel Identification System (LPIS) data. It is a vector layer, provided by Ministry of Agriculture and it is available on the Public Land Registry portal (LPIS, 2018) as web based browser. For the purpose of this thesis, the complete data covering the entire Czech Republic in a separate dataset was requested at Department of Land Use and Improvement in Czech University of Life Sciences. Obtained datasets covered three-year period (2015 – 2017). One of its main purposes is to explore and identify agricultural production block attributes within whole Czech Republic.

To achieve the goal of this study, it was important to be able to compare organic fields with conventional fields, using set of specific parameters such as management type, field type, location, elevation, slope, orientation, area and surface temperature. Some of those parameters are included in LPIS data (management type, field type, location, elevation, slope, area) and some had to be calculated (orientation, surface temperature).

To obtain all named relevant data for such a comparative analysis, few following steps needed to be done.

4.3.1 Data preparation

Data have been available in 3 separated datasets - year 2015, 2016 and 2017. As an initial step, it was necessary to prepare them for purpose of this study. LPIS vector layer originally contains a lot of information, has its specific coordinate system and covers the entire territory of the Czech Republic. As in the previous steps, all processes were performed in the *ArcGIS 10.4* program.

Unification of coordinate systems

Before any further analysis could begin, it was necessary to unify the coordinate systems of calculated thermal images and LPIS vector layer. All Landsat imagery is standardly provided in World Geodetic System (WGS 1984) coordinates and Universal Transverse Mercator (UTM) projection (U.S. Department of Interior, 2013). It is also important to count on a particular UTM zone of particular image, because every zone

has different distortion of projection. This information is included in metadata file of every single Landsat image. For images, used it this analysis, the UTM zone is 33N (basic meridian = 15°; northern hemisphere). On the other side, in case of LPIS vector data, basic coordinate system is Datum of Uniform Trigonometric Cadastral Network (in Czech: S-JTSK) and Krovak East North projection (basic meridian is Greenwich).

As the work coordinate system was selected WGS 1984 (the one in which the satellite data is). To transform LPIS layer into the same system was used *Project* tool (*Geoprocessing → ArcToolbox → Data Management Tools → Projections and Transformations → Project*). As input coordinate system was selected *S-JTSK_Krovak_East_North* and as output *WGS_1984_UTM_Zone_33N*.

Defining an area of interest

As mentioned above, the scope of this study is more or less northern and central part of Bohemia (*Figure 2*). This area is defined by position and dimension of used Landsat images. That is why it was needed to reduce the LPIS layer. For this purpose was

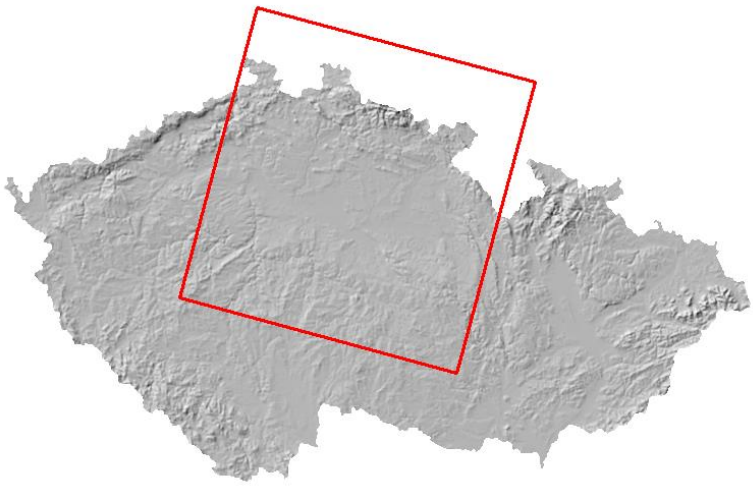

Figure 2: *Visualization of studied area*

created new polyline layer and manually drawn quadrangular vector shape which runs directly around the circumference of the Landsat image. Right after was used *Clip* tool (*Geoprocessing → Clip*) and as a clip feature was utilized this newly created polyline shape.

Detailed data sorting

After defining the exact area of interest, a detailed sorting of data has come to pass. Firstly, the attribute table of LPIS layer has too many attributes and only few of them are relevant for this analysis. To simplify the dataset, useless columns were turned off by function *Turn Field Off*. Only fields *OBJECTID* (field identification number), *VYSKA* (field mean elevation in meters), *SVAZITOST* (field mean slope in %), *EKO* (management type on field), *KULTURANAZ* (field type), *KULTURAKOD* (field code), *Shape_Length* (field circumference in meters) and *Shape_Area* (field area in square meters) were retained.

Next step was to allocate fields which do not match the required analysis parameters and delete them. By using *Select By Attributes* tool, usable fields were selected and the rest was deleted. As decisive parameters were chosen:

- **Minimum area** – as minimum field area that can come into assessment is 900 m^2 with respect of thermal images ground resolution. The reason is that the area of 1 thermal image pixel is 30 m × 30 m (= 900 m^2). All fields bellow this boundary, were deleted.

- **Adequate shape** – because some fields may meet the condition of minimum area, but can have completely inappropriate shape (e.g. too narrow), this condition was established. To determine and separate improper fields, the shape ratio was used. It was calculated by following command: "*(Shape_Area / Shape_Length) < 7.5"*. The reason is that one single thermal image pixel has the ratio 7.5 (area = 900 m^2; circumference = 120 m), so all fields which had lower ratio, were deleted.

- **Field type** – the field type that is in scope of this study is arable land. All the others (e.g. grassland, pond, orchard etc.) were deleted.

- **Field management** – in LPIS data is also included information about the type of management. The information is mediated by these codes: *0* - conventional management; *1* - organic management; *2* – transitional period; *3*, *4*, *5*, *6* – uncertain status. In respect to this parameter, only conventional (code 0) and organic (code 1) fields are suitable. The others were deleted.

- **Cloud cover** – when estimating land surface temperature (LST) by use of satellite imagery, clouds in atmosphere cause troubles and uncertainty in results. For that reason it was necessary to remove fields, covered by clouds for every thermal image separately. As an ideal option was chosen *Select by Polygon* selection tool. Clouds were manually traced by selection polygon and the fields falling inside the shape, were deleted for every single thermal image separately.

Additional parameters

For the purposes of this analysis, it was necessary to derive even more variables that come into the final evaluation: aspect (i.e. field orientation), location of individual fields and the most important – land surface temperature (LST).

- **Aspect** – this parameter is very important for matching parcels of the same orientation. The difference of geographical orientation of the field could have major impact on the resulting LST.

  As a background data, within area of interest, the Digital Terrain Model of the Czech Republic of the 5th generation (DMR 5G) was used. It is raster data layer, in which every pixel has 2 × 2 meters resolution and which is originally provided in S-JTSK - Krovak coordinate system (ČÚZK, 2013). For this reason it was convenient to resample the raster into lower resolution (30 × 30 meters) by using *Aggregate* tool (*Geoprocessing → ArcToolbox → Spatial Analyst Tools → Generalization → Aggregate*). Another approach was to project the model into current coordinate system (WGS_1984_UTM_Zone_33N) using *Project* tool (*Geoprocessing → ArcToolbox → Data Management Tools → Projections and Transformations → Project*).

  After all these preparations, the aspect value itself was calculated by *Aspect* tool (*Geoprocessing → ArcToolbox → Spatial Analyst Tools → Surface → Aspect*).

  To assign aspect value for every single field, the *Zonal Statistics as Table* tool (*Geoprocessing → ArcToolbox → Spatial Analyst Tools → Zonal → Zonal Statistics as Table*) was used with *MEAN* value.

- **Field location** – polygon centroids were used to determine approximate location of the field. For obtaining these values was used *Calculate*

Geometry tool (*Attribute Table → Add Field… → Calculate Geometry…*), where are options to calculate *X Coordinate of Centroid* and *Y Coordinate of Centroid*.

- **Land surface temperature** – land surface temperature (LST) is crucial variable for determining the differences between organic and conventional fields. So that this could be done, average LST value was calculated for every field from previously obtained thermal images. Same as in filed location part, the *Calculate Geometry* tool was utilized, with *MEAN* value entered into calculation.

Redefined LPIS layer

The newly modified polygonal LPIS layer was prepared for subsequent comparative analysis. All required parameters are calculated or derived in *Attribute Table*. These parameters are:

- *OBJECTID* - parcel identification number
- *ELEVATION* – average parcel altitude [*m a.s.l.*]
- *ASPECT* – average parcel orientation towards cardinal directions [°]
- *SLOPE* – average parcel slope [*%*]
- *AREA* – area of parcel [m^2]
- *X_CENT* – X coordinate of polygon centroid
- *Y_CENT* – Y coordinate of polygon centroid
- *EKO* – classification of used management (0 = conventional; 1 = organic)
- *LST* – average temperature on the parcel surface [°*C*]

All the attribute tables were exported as *TXT* files to allow computational script to load them.

4.4 Pairing algorithm

After all the previous calculations and data preparations, next step was to create specific dataset, where every organic parcel will be distributed with corresponding conventional one. In other words - for every organic field it was needed to find conventional field that meets the selection criteria based on specified parameters.

To achieve this goal the *MATLAB 2017a* software was used and the computational *Parcel Pairing Script* (*Appendix 1*) was developed there. The structure of the calculation was created as follows (*Figure 3*):

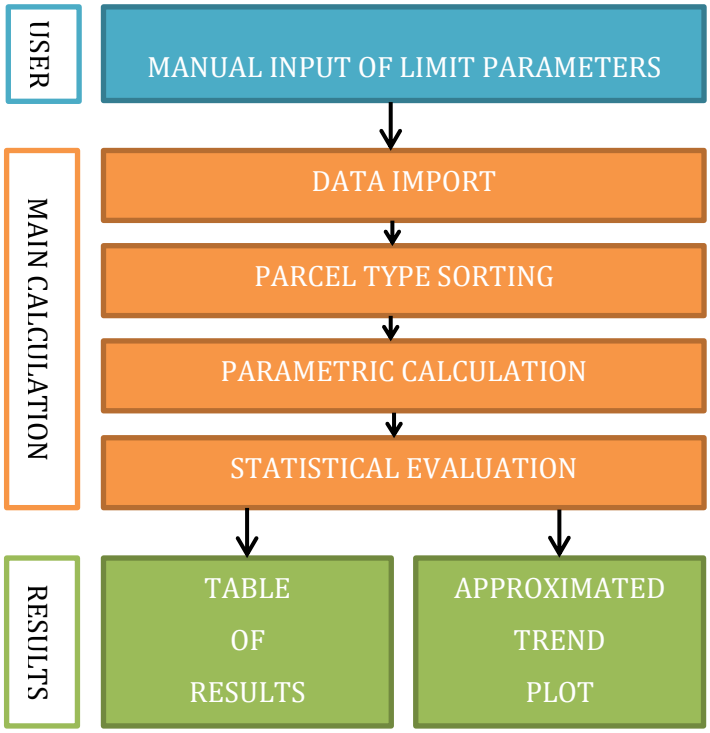

Figure 3: *The computational structure of Parcel Pairing Script*

where:

- **Manual input of limit parameters** – in this part the user must manually enter the limitations on the basis of which for every organic field (i.e. parcel) is searched matching conventional one. Searching parameters are: *DISTANCE limit*, *ELEVATION limit*, *ASPECT limit*, *SLOPE limit* and *AREA limit*. Another parameter which is manually entered by the user is *Degree of polynomial approximation*. It determines the order of used approximation polynomial. Manually used limits are showed in the table below (*Table 2*).

Table 2: *Values of the searching limits that were used in the calculation in Parcel Pairing Script*

Manually entered searching limits					
DISTANCE limit [*m*]	**ELEVATION limit [*m*]**	**ASPECT limit [°]**	**SLOPE limit [%]**	**AREA limit [%]**	**Order of approximation polynomial**
± 2000	± 100	± 60	± 1	± 30	8

- **Data import** – here are all attribute tables in text format automatically imported into matrixes.

- **Parcel type sorting** – as was mentioned above (*Data preparation* chapter), every parcel has its own code – "1" or "0" (1 = organic management; 0 = conventional management). Based on this distinction are parcels sorted and put into 2 different groups (organic and conventional).

- **Parametric calculation** – within this part of the script runs the main calculation that is responsible for proper pairing of individual parcels. In basic terms, for every organic parcel is found the set of all conventional "candidates", which are meeting searching limits and then it choose the closest one on the *Distance limit* basis.

- **Statistical evaluation** – in this part the code is working only with newly established parcel pairs. It statistically evaluates the significance of land surface temperature (LST) differences, using *Paired T-test*.

- **Table of results** – the first part of the script´s outcome is table of results, where are information such as *Number of found organic parcels (ALL, USED, SKIPPED)*, *Mean value of LST*, *Statistical evaluation (standard deviation, p-value)* and so on.

- **Approximated trend plot** – the second part of results is the plot, where over 3-year period are illustrated two interconnected information: (i) mean values of LST differences (in the form of columns) and (ii) the trend of LST fluctuation in time (in the form of approximation Legendre´s polynomial).

5. Results

The outcome of this thesis is relatively diverse. For this reason, this chapter is divided into three related units: (i) processing of satellite images, (ii) pairing and calculations made by Parcel Pairing Script and (iii) statistical evaluation of results.

5.1 Thermal image processing

Entire satellite image processing (geo-referencing, calculations, cloud clearing etc.) was done in *ArcGIS 10.4* software. Some of downloaded images were immediately discarded due to the high cloud cover or inappropriate cloud distribution over scene. In cases, where clouds were relatively compact, it was possible to remove them manually. But if the distribution of clouds was enormously irregular and fragmented (*Fig. 4*), it was necessary to exclude such images from analysis in order to avoid high inaccuracies in the subsequent calculation.

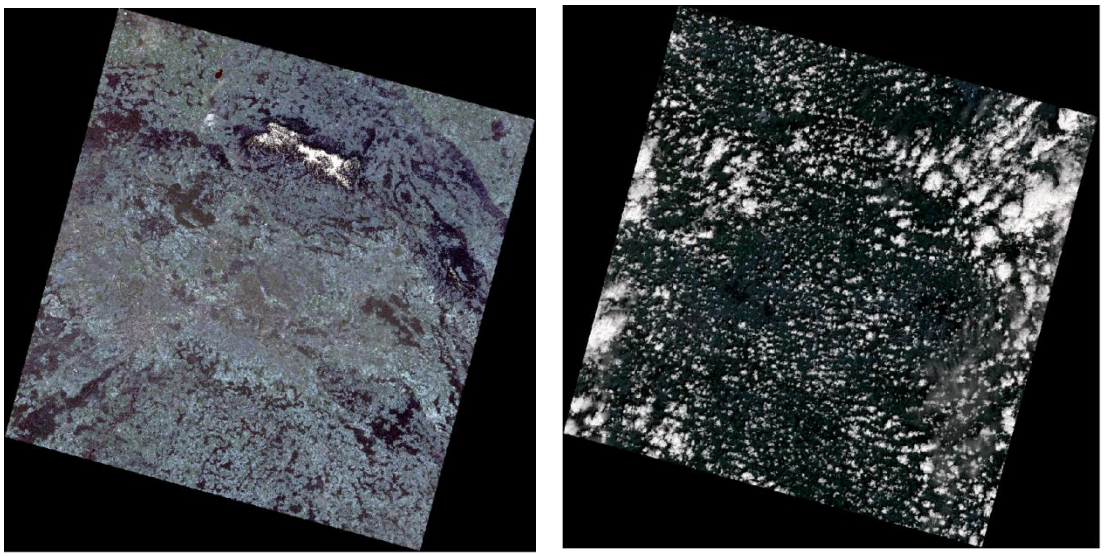

Figure 4: *Example of analysis-suitable image (on the left) and analysis-non-suitable image (on the right)*

After this "cleaning process" 19 images in total remained in the analysis – 7 images for year 2015, 4 images for year 2016 and 8 images for year 2017. On every single image was done several-step calculation to retrieve the land surface temperature (LST).

Final thermal images were exported into *geo-TIFF* format, which provides zero compression and information about geographical reference of image.

As a next step, the LPIS vector layer, containing parcel outline and other information, was added. LPIS layer was transformed into the same geographical coordinate system as images (*WGS_1984_UTM_Zone_33N*) to fit the datasets (*Fig. 5*).

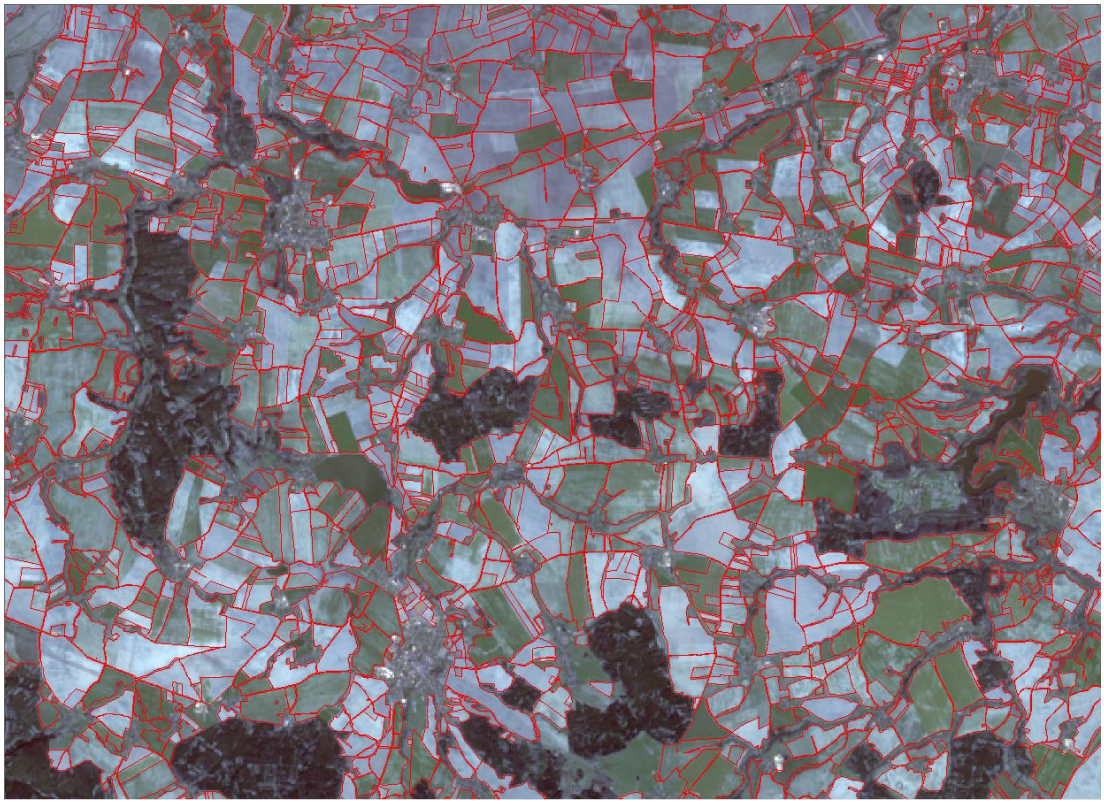

Figure 5: *Geo-referenced LPIS layer on the true color satellite image*

After that, the parcels covered by clouds were manually deleted from vector dataset over every single scene. Because there is a different level of cloud cover on every image, each one has different number of usable parcels in the calculation (*Tab. 4*). This leads to the fact that the number of parcels may considerably vary from image to image (*Fig. 6*).

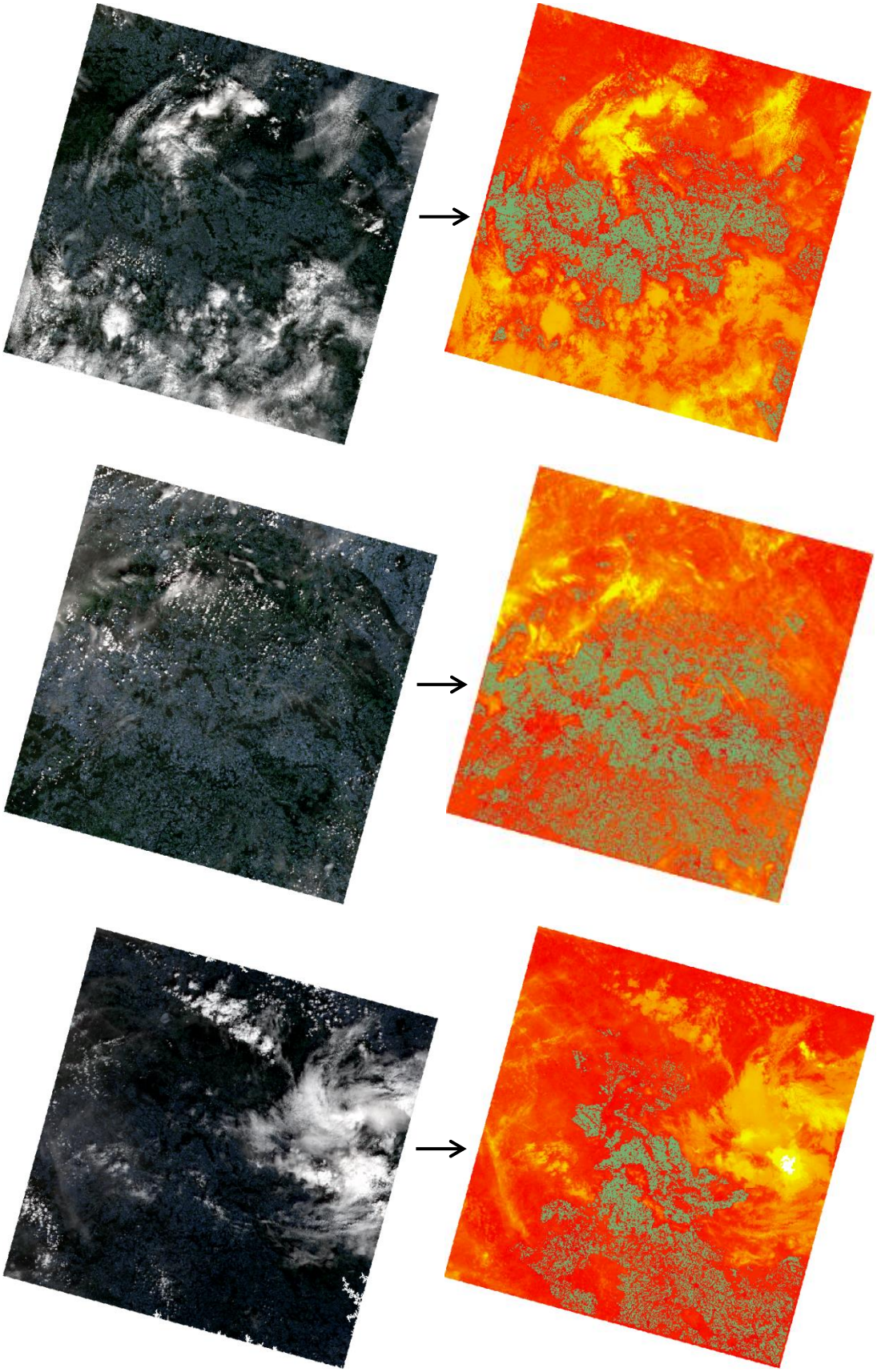

Figure 6: *Examples of 3 image pairs – true color image (on the left) and thermal image (on the right). Parcels are marked on thermal images (green). The difference in parcel number is clearly visible.*

From that moment, the calculation of mean LST of each parcel could have started. This task was made by *Zonal Statistics as Table* tool. This tool takes the value of every pixel that falls into the parcel´s perimeter (*Fig. 7*) and calculate the *MEAN* value.

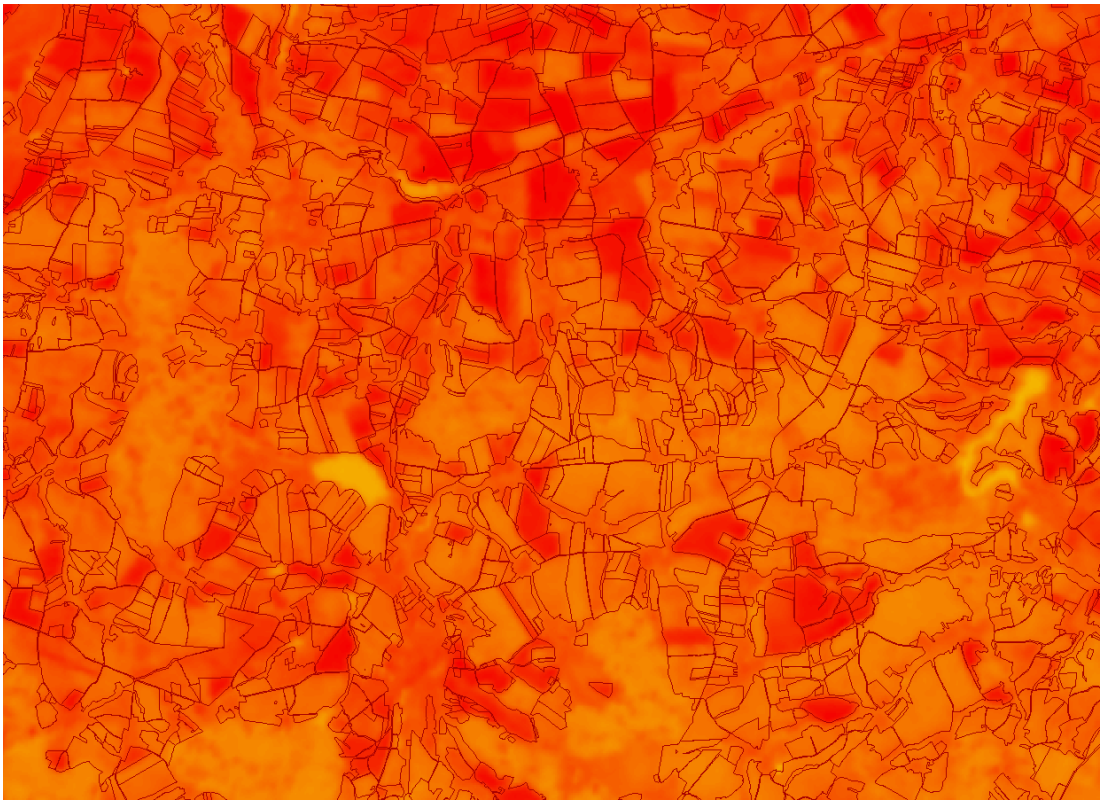

Figure 7: *Parcel vector layer over thermal image (in detail)*

Calculated mean LST value of each parcel was added to the *Attribute Table* (*Tab. 3*) of vector layer. At the end, the table was exported into text file, so the data could be loaded into the computational script.

Table 3: *Sample polygon Attribute Table*

FID	Shape *	OBJECTID	ELEVATION	ASPECT	SLOPE	AREA	X_CENT	Y_CENT	EKO	LST
0	Polygon	618	447,05	171,7	5,3	184775,06	416377,084519	5524985,764049	0	-1,7
1	Polygon	619	438,29	171,9	4,3	103022,27	416870,947198	5525014,219922	0	-1,3
2	Polygon	995	389,73	121,3	2	8843,99	416897,621447	5523677,172158	0	-0,2
3	Polygon	1822	384,43	97	1,7	147167,73	416969,471293	5523369,823088	0	0,3
4	Polygon	2004	423,56	59	2,7	252261,83	416792,92157	5519185,464067	1	-2,9
5	Polygon	2046	394,98	266,8	1,2	21262,96	419043,587982	5521264,190574	0	0,8
6	Polygon	2429	406,76	131	2,2	127394,29	416169,763101	5523878,331957	0	-0,6
7	Polygon	3614	392,24	113,5	2,2	37764,01	417248,037462	5524230,940408	0	0,1
8	Polygon	4017	490,97	30,9	3,5	172214,64	419935,755046	5518269,45309	0	-3,2
9	Polygon	4048	433,57	176	3	616793,05	417285,82083	5518545,198127	0	-4
10	Polygon	4530	413,44	187,8	2,3	342230,91	417310,661506	5519507,936063	0	-2,7
11	Polygon	4713	469,23	98,5	5,9	9121,26	416478,844571	5516892,684447	0	-2,8
12	Polygon	4991	505,57	43,3	4,1	3442,03	416109,302968	5516597,508148	0	-4,3
13	Polygon	5322	524,44	97,6	2,4	40400,27	412491,396513	5512621,661583	0	-4,7
14	Polygon	5391	421,24	122,6	2,5	204033,67	417391,371582	5519196,461719	1	-2,3
15	Polygon	5450	449,05	119,2	4,9	22236,31	418095,989268	5516929,210118	0	-3
16	Polygon	5710	383,21	308,5	3,3	208218,99	418582,602985	5522529,949629	0	-0,3
17	Polygon	6833	406,27	220,7	3	30287,31	417844,445426	5519480,972316	0	-3,3
18	Polygon	7021	525,44	230,4	3,1	79558,28	410843,717385	5510449,075171	0	-5,2
19	Polygon	7047	402,18	145,9	2,2	73337,75	417814,447613	5520105,588079	0	-2,5
20	Polygon	7058	439,58	138	3,5	48513,53	416517,080808	5518294,908107	0	-5,8

5.2 Paired parcels and final trend

The main part of the analysis was to find pairs of parcels (organic and conventional) based on manually entered searching parameters (*Tab. 2*). For this purpose was developed Parcel Pairing Script (*Appendix 1*) in *MATLAB 2017a*. The outcome of this script is the table (*Tab. 4*) containing various information such as: *Date* (acquisition date of image), *ALL organic parcels* (number of organic parcels within each scene), *USED organic parcels* (number of parcels which met the searching criteria), *SKIPPED organic parcels* (number of parcels which didn´t meet the searching criteria), *DIST. > lim* (parcels skipped due to exceeding the distance limit), *OTHER > lim* (parcels skipped due to exceeding any other limit) and *Mean LST differ. [°C]* (mean LST difference, calculated from USED parcels, pairs respectively).

Table 4: *The overview table of used (i.e. successfully paired) organic parcels*

Satellite image ID	Year	Date	ALL organic parcels	USED organic parcels	SKIPPED organic parcels	DIST. > lim	OTHER > lim	Mean LST differ. [°C]
1	2015	06/JAN	1074	**541**	533	22	1052	**0,2**
2		07/FEB	1992	**979**	1013	106	1886	**0,1**
3		01/JUL	1398	**634**	764	83	1315	**0,6**
4		17/JUL	1531	**818**	713	65	1466	**0,4**
5		03/SEP	863	**389**	474	86	777	**-0,1**
6		19/SEP	1861	**905**	956	114	1747	**-0,4**
7		05/OCT	823	**415**	408	36	787	**-0,4**
8	2016	26/FEB	825	**447**	378	7	818	**0,2**
9		30/APR	1867	**915**	952	152	1715	**0,4**
10		04/AUG	1543	**800**	743	36	1507	**-0,4**
11		07/OCT	280	**140**	140	6	274	**0,2**
12	2017	27/JAN	2022	**987**	1035	134	1888	**0,0**
13		16/MAR	1794	**861**	933	114	1680	**0,1**
14		01/APR	2039	**993**	1046	135	1904	**0,2**
15		19/MAY	2140	**1039**	1101	135	2005	**0,4**
16		20/JUN	2101	**1024**	1077	136	1965	**0,5**
17		22/JUL	1129	**600**	529	6	1123	**0,1**
18		07/AUG	1277	**594**	683	120	1157	**-0,4**
19		13/DEC	1437	**759**	678	25	1412	**0,1**

Another outcome is the 3-year trend of LST differences fluctuation in time (*Fig. 8*). It is visible, that there exists relatively high repeating tendency of LST differences between organic and conventional fields.

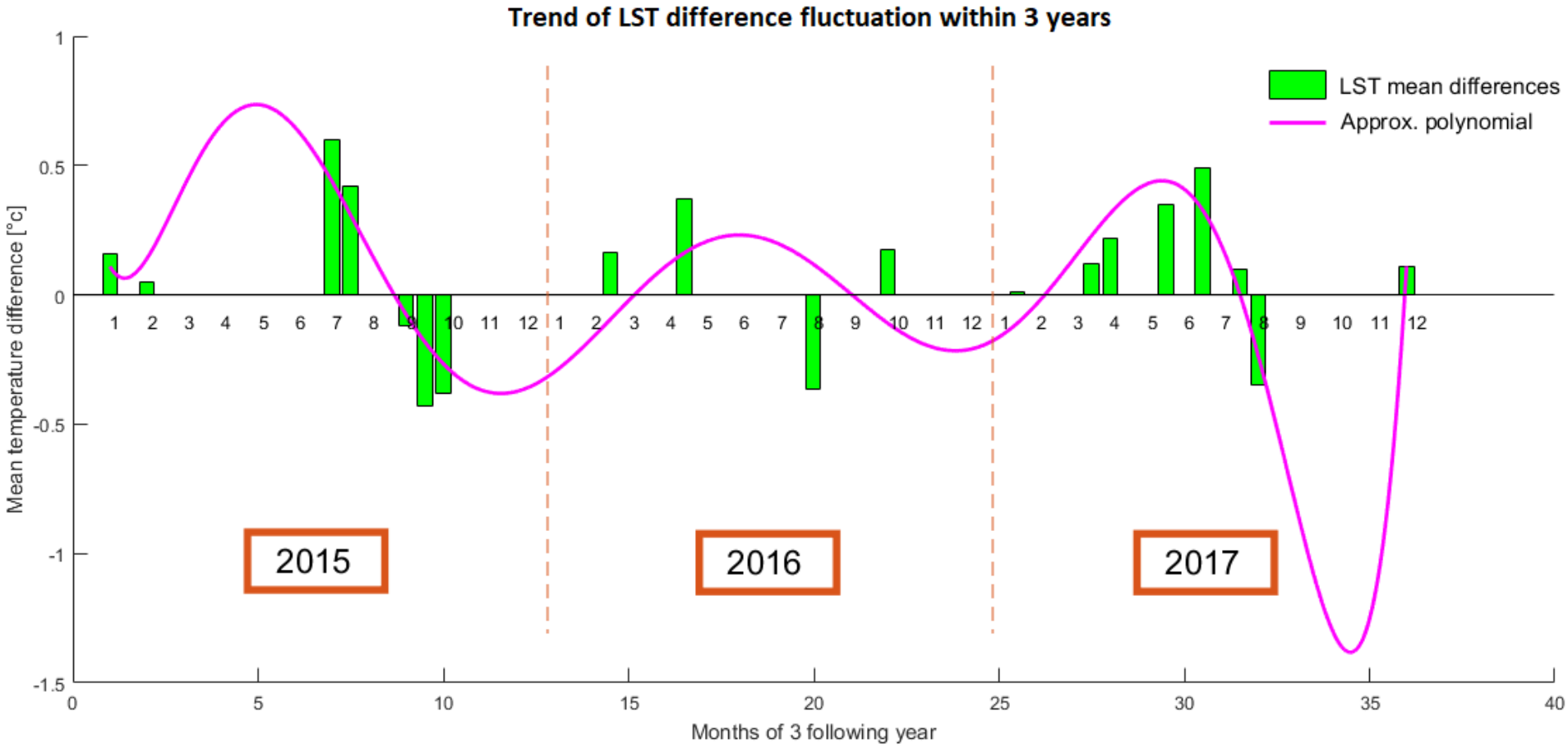

Figure 8: *The plot, generated in Parcel Pairing Script, which represents the 3-year trend in LST difference fluctuation in time between organic and conventional fields. On the X axes is calculated mean LST difference, on the Y axes are months. As higher mean LST difference is, as warmer organic field is (and opposite). For the approximation (purple line) is used Legendre´s polynomial of 8th order.*

5.3 Statistics

In order to get higher data validity, the results were statistically tested. As suitable statistical assessment was used *Two-sided Paired T-test*, with the Confidence interval 95%. One of the main T-test assumptions, the normality of the data, was met (*Fig. 9*). As the null (H_0) and alternative (H_1) hypotheses were determined:

$H_0 = "mean\ LST\ difference = 0"$

$H_1 = "mean\ LST\ difference \neq 0"$

The statistical evaluation for every single image was calculated in *Parcel Pairing Script* and is illustrated in the table (*Tab. 5*).

Table 5: *Table of LST difference statistical evaluation of every image*

Satellite image ID	Year	Date	USED organic parcels	Hypothesis	Statistically significant? (conf. Int. 95%)	*p*-value	Mean LST difference [°C]	Mean LST diff. standard deviation [°C]
1	2015	06/JAN	541	1	YES	**0,005**	0,2	1,4
2		07/FEB	979	0	NO	**0,115**	0,1	0,9
3		01/JUL	634	1	YES	**0,003**	0,6	5,1
4		17/JUL	818	1	YES	**0,006**	0,4	4,4
5		03/SEP	389	0	NO	**0,466**	-0,1	3,3
6		19/SEP	905	1	YES	**0,000**	-0,4	2,5
7		05/OCT	415	1	YES	**0,000**	-0,4	2,1
8	2016	26/FEB	447	0	NO	**0,074**	0,2	2,3
9		30/APR	915	1	YES	**0,000**	0,1	2,8
10		04/AUG	800	1	YES	**0,000**	-0,2	2,8
11		07/OCT	140	0	NO	**0,516**	0,1	3,7
12	2017	27/JAN	987	0	NO	**0,782**	0,0	0,7
13		16/MAR	861	1	YES	**0,003**	0,1	1,3
14		01/APR	993	1	YES	**0,000**	0,1	1,8
15		19/MAY	1039	1	YES	**0,000**	0,2	2,6
16		20/JUN	1024	1	YES	**0,000**	0,5	3,0
17		22/JUL	600	0	NO	**0,161**	0,1	1,8
18		07/AUG	594	1	YES	**0,012**	-0,2	3,3
19		13/DEC	759	1	YES	**0,000**	0,1	0,6

Second statistical outcome, generated in *Parcel Pairing Script*, was the trend plot with mean LST differences, distinguished in terms *"significant"* or *"non-significant"* (*Fig. 10*).

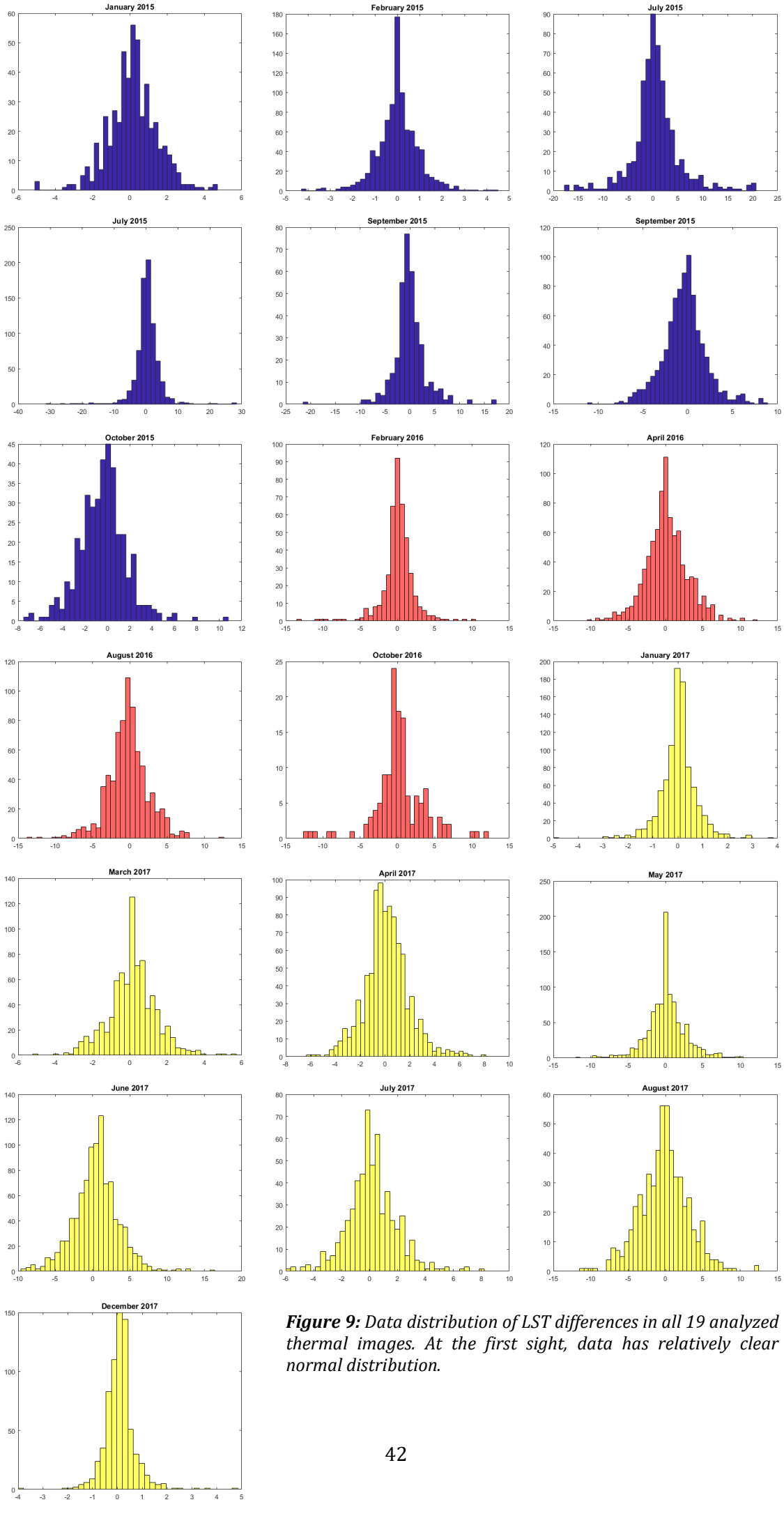

Figure 9: *Data distribution of LST differences in all 19 analyzed thermal images. At the first sight, data has relatively clear normal distribution.*

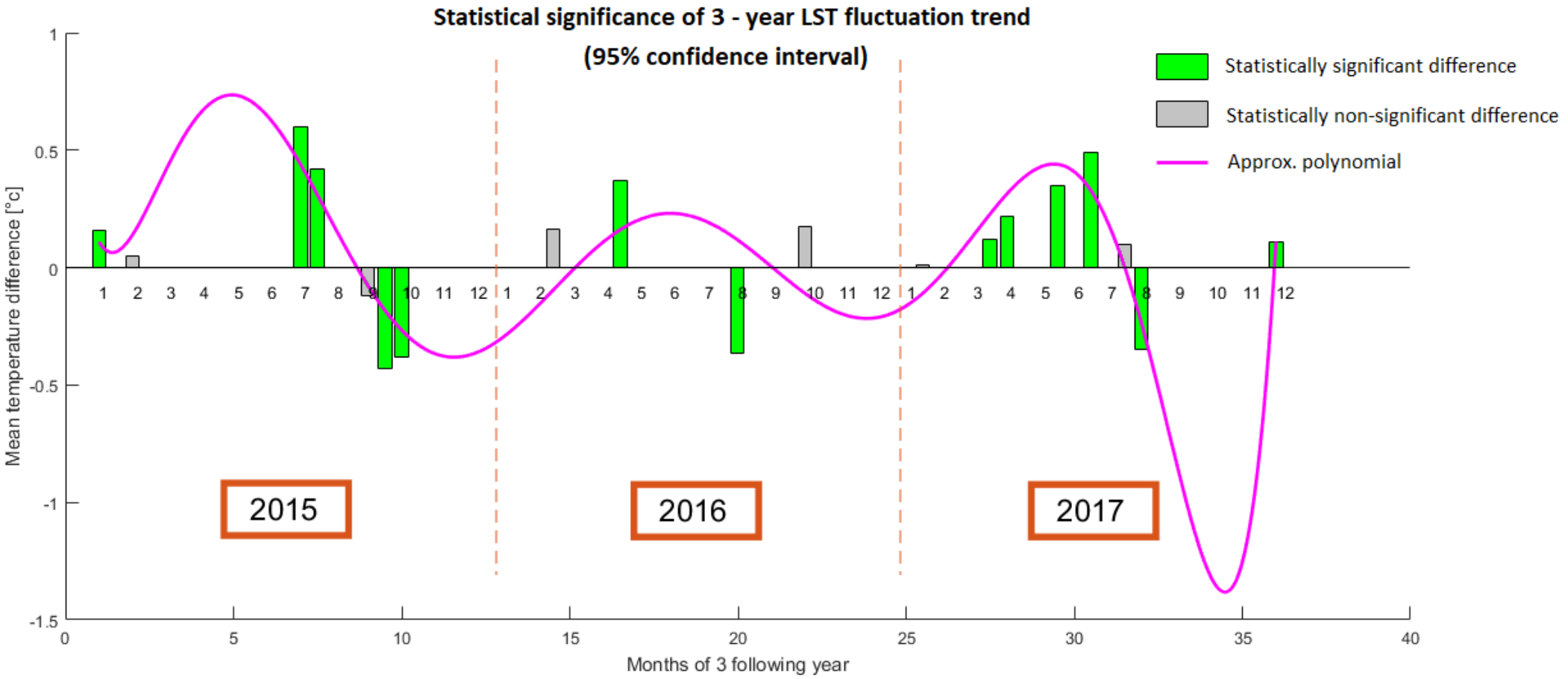

Figure 10: *The plot, illustrating which LST differences are statistically significant (green) and which are non-significant (grey) in 95% confidence interval.*

6. Discussion

Analyzing the earth surface with satellite imagery tends to be more widespread used literally day after day. A large number of parameters can be monitored by remote sensing. The land surface temperature (LST) is one of them. From my point of view, there are hardly any studies to deal with the influence of chosen agricultural management on LST. In my thesis, I´ve tried to find such a correlation.

Based on the results it is evident that some LST differences between organic and conventional fields are present and even that the repetitive trend in these differences actually exists (*Fig. 8*). The final approximation shows that LST on organic fields tends to be higher during spring and summer (from March to August) and lower during fall and winter (from September to February). As usual, while monitoring any long-term trend, also here are some contradictions. Especially in tested year 2016 the higher deviation of LST differences from approximation curve is visible. The problem was lower number of usable images and relatively high and uneven cloud cover. So that we could declare the data in year 2016 as similarly valid as other years, we would need at least twice as many usable images and involve them into the calculation.

Another thing that is needed to be taken into account is the fact that entire calculation of thermal images is loaded by many inaccuracies. Positive fact is that when it comes to differences comparison, many inaccuracies are cut off. Despite that, it is needed to pay special attention to land surface emissivity (LSE) estimation. Parastatidis et al. (2017) demonstrates that accuracy of LSE determination directly affects the LST final accuracy. It is clear that the level of precision, while estimating LSE, is absolutely essential. For my analysis I´ve chosen NDVI-based method, which is very often used and achieves relatively good results (Yu et al., 2014). However, it has also its own limitations. NDVI-based method is sensitive on the amount of vegetation cover, but it can barely recognize specific crop type (Karnieli et al., 2010).

Next calculation-based issue was finding the trend – i.e. approximation. In this thesis I used Lagendre´s polynomial of 8th order. Number of orders is used on the basis of number of expected peaks in the curve. It seemed to me as an appropriate choice, but it has, like any other function, its limitations. According to Gambino and Kock (2013), Lagendre´s polynomial is characterized by the fact that the approximation is more

steep at the edges of monitored trend. This is happening because of the absence of any value going behind both ends (left and right) of studied dataset. It can be thus assumed that if I would have used also data from second half of year 2014 (on the left end) and first half of year 2018 (on the right end), the overall course of approximation function would be smoother and within monitored 3-year period also more valid.

In order to declare any data as relevant, it is always needed to test them by some statistical approach. I´ve used *Two-sided Paired T-test*, because the data structure was appropriate and also the assumption of normality of the data was met (*Fig. 9*). When looking at the statistical results, except one case (August 2016), all statistically significant differences confirm the trend. One might argue that there are more non-significant results, but majority of them (4 of 6; February 2015, September 2015, January 2017 and July 2017) are logically not significant due to their small mean value. Because of they are in spots, where LST should be at minimum difference, it again confirms the repetitive fluctuation trend.

At the end of this work I would like add that the ever increasing importance of finding the solutions how to feed the world in the most sustainable way is the reason, why the comparison of organic and conventional farming is becoming more and more frequent. Organic farming has, without any question, many well studied advantages over conventional one (Hilmi, 2012). However, while comparing properties of these two agricultural systems and taking into account only physical relationship between agriculture and environment, absolute majority of studies done are focused on the impact, caused by environment (weather, global change, precipitation etc.) and affecting the agriculture (yield decrease, economic losses etc.). This prompts the question, if there are enough critical and objective researches assessing the physical impact of agriculture on the environment. I am afraid there are very few. Agriculture and the environment are two communicating vessels – healthier agriculture means healthier environment and vice versa. For these reasons, I hope that my thesis will help to equalize this disbalance at least a little and will provide the basis for further research on this topic.

7. Conclusion

In this thesis I have analyzed the relationship between the type of agricultural management (organic and conventional) and land surface temperature using the remote sensing method within 3-year period (2015 – 2017) on agricultural fields in the territory of northern and central Bohemia. Based on available input data (Landsat 8 satellite images; LPIS vector layer), I have processed and calculated the thermal images, with which I have tried to find out, if there is some repetitive trend in land surface temperature fluctuation on these fields. In order to achieve this, the computational script (*Parcel Pairing Script*) has been developed and properly used. All results have been statistically tested in order to gain outcome with relevant validity. The objectives of this thesis were thus accomplished.

Regarding the results, it turned out that some temperature fluctuation trend, with relatively high probability, really exists. The temperature difference approximation, projected through 3 following years, showed that organic field is on its surface warmer during spring and summer (from March to August) and cooler during autumn and winter (from September to February). The surface temperature difference fluctuation seems to be around ± 0,7°C, depending on current season. The trend isn´t so strong in year 2016, but this can be probably caused due to insufficient number of suitable images and its questionable validity.

Whereas the interest in organic farming is growing as a result of the need for worldwide sustainable development solutions, ongoing hand in hand with widening the interdisciplinary range of remote sensing technologies use, further study of agricultural processes and its impacts on the environment should be the concern. Also because of that I believe, that this thesis will help uncover another piece in puzzle.

8. References

Agam, N., Kustas, W.P., Anderson, M.C., Li, F., Neale, C.M.U., 2007. A vegetation index based technique for spatial sharpening of thermal imagery. Remote Sens. Environ. 107, 545–558. https://doi.org/10.1016/j.rse.2006.10.006

Barsi, J.A., Barker, J.L., Schott, J.R., 2003. An Atmospheric Correction Parameter Calculator for a single thermal band earth-sensing instrument. IEEE Int. Geosci. Remote Sens. Symp. 2003 0, 2–4. https://doi.org/10.1109/IGARSS.2003.1294665

Barsi, J.A., Lee, K., Kvaran, G., Markham, B.L., Pedelty, J.A., 2014. The spectral response of the Landsat-8 operational land imager. Remote Sens. 6, 10232–10251. https://doi.org/10.3390/rs61010232

Barsi, J.A., Schott, J.R., Palluconi, F.D., Hook, S.J., 2005. Validation of a web-based atmospheric correction tool for single thermal band instruments 5882, 58820E. https://doi.org/10.1117/12.619990

Brožová, I., Beranová, M., 2017. Agris on-line Papers in Economics and Informatics A Comparative Analysis of Organic and Conventional Farming Profitability IX, 3–16. https://doi.org/10.7160/aol.2017.090101.Introduction

Carlson, T.N., Ripley, D.A., 1997. On the relation between NDVI, fractional vegetation cover, and leaf area index. Remote Sens. Environ. 62, 241–252. https://doi.org/10.1016/S0034-4257(97)00104-1

ČÚZK, 2013. Digital Terrain Model of the Czech Republic of the 5th generation (DMR 5G).

Department of Economic and Social Affairs. Population Division., 2017. World Population Prospects: The 2017 Revision, United Nations. https://doi.org/10.1017/CBO9781107415324.004

Dytrtová, K., Šarapatka, B., Opršal, Z., 2016. Does organic farming influence landscape composition? Two cases from the Czech Republic. Agroecol. Sustain. Food Syst. 40, 714–735. https://doi.org/10.1080/21683565.2016.1186131

EEA, 2017. Annual European Union greenhouse gas inventory 1990–2015 and inventory report 2017. Annu. Eur. Union Greenh. gas Invent. 1990–2015 Invent. Rep. 2017 — Eur. Environ. Agency.

El-Zeiny, A.M., Effat, H.A., 2017. Environmental monitoring of spatiotemporal change in land use/land cover and its impact on land surface temperature in El-Fayoum governorate, Egypt. Remote Sens. Appl. Soc. Environ. 8, 266–277. https://doi.org/10.1016/j.rsase.2017.10.003

Fahnestock, M., Scambos, T., Moon, T., Gardner, A., Haran, T., Klinger, M., 2016. Rapid large-area mapping of ice flow using Landsat 8. Remote Sens. Environ. 185, 84–94. https://doi.org/10.1016/j.rse.2015.11.023

Fathizad, H., Tazeh, M., Kalantari, S., Shojaei, S., 2017. The investigation of spatiotemporal variations of land surface temperature based on land use changes using NDVI in southwest of Iran. J. African Earth Sci. 134, 249–256. https://doi.org/10.1016/j.jafrearsci.2017.06.007

Firbank, L.G., Petit, S., Smart, S., Blain, A., Fuller, R.J., 2008. Assessing the impacts of agricultural intensification on biodiversity: a British perspective. Philos. Trans. R. Soc. B Biol. Sci. 363, 777–787. https://doi.org/10.1098/rstb.2007.2183

Foley, J.A., Ramankutty, N., Brauman, K.A., Cassidy, E.S., Gerber, J.S., Johnston, M., Mueller, N.D., O'Connell, C., Ray, D.K., West, P.C., Balzer, C., Bennett, E.M., Carpenter, S.R., Hill, J., Monfreda, C., Polasky, S., Rockström, J., Sheehan, J., Siebert, S., Tilman, D., Zaks, D.P.M., 2011. Solutions for a cultivated planet. Nature 478, 337–342. https://doi.org/10.1038/nature10452

Fra??kov??, E., Cattaneo, C., 2017. Organic farming in the past and today: sociometabolic perspective on a Central European case study. Reg. Environ. Chang. 1–13. https://doi.org/10.1007/s10113-016-1099-8

Fu, B., Burgher, I., 2015. Riparian vegetation NDVI dynamics and its relationship with climate, surface water and groundwater. J. Arid Environ. 113, 59–68. https://doi.org/10.1016/j.jaridenv.2014.09.010

Gambino, N., Kock, J., 2013. Polynomial functors and polynomial monads. Math. Proc. Cambridge Philos. Soc. 154, 153–192. https://doi.org/10.1017/S0305004112000394

Giampietro, M., Mayumi, K., Şorman, A.H., 2013. Energy analysis for a sustainable future: Multi-scale integrated analysis of societal and ecosystem metabolism, Energy Analysis for a Sustainable Future: Multi-Scale Integrated Analysis of Societal and Ecosystem Metabolism. https://doi.org/10.4324/9780203107997

Gomiero, T., Pimentel, D., Paoletti, M.G., 2011. Environmental Impact of Different Agricultural Management Practices: Conventional vs. Organic Agriculture. CRC. Crit. Rev. Plant Sci. 30, 95–124. https://doi.org/10.1080/07352689.2011.554355

Hansen, J., Ruedy, R., Sato, M., Lo, K., 2010. Global surface temperature change. Rev. Geophys. 48. https://doi.org/10.1029/2010RG000345

Herb, W.R., Janke, B., Mohseni, O., Stefan, H.G., 2008. Ground surface temperature simulation for different land covers. J. Hydrol. 356, 327–343. https://doi.org/10.1016/j.jhydrol.2008.04.020

Hilmi, A., 2012. Agricultural transition, The More and Better Network. The More and Better Network.

Hole, D.G., Perkins, A.J., Wilson, J.D., Alexander, I.H., Grice, P. V., Evans, A.D., 2005. Does organic farming benefit biodiversity? Biol. Conserv. https://doi.org/10.1016/j.biocon.2004.07.018

Hulley, G.C., Hook, S.J., Abbott, E., Malakar, N., Islam, T., Abrams, M., 2015. The ASTER Global Emissivity Dataset (ASTER GED): Mapping Earth's emissivity at 100 meter spatial scale. Geophys. Res. Lett. 42, 7966–7976. https://doi.org/10.1002/2015GL065564

Chandra, A., McNamara, K.E., Dargusch, P., 2017. Climate-smart agriculture: perspectives and framings. Clim. Policy 0, 1–16. https://doi.org/10.1080/14693062.2017.1316968

Chiriacò, M.V., Grossi, G., Castaldi, S., Valentini, R., 2017. The contribution to climate change of the organic versus conventional wheat farming: A case study on the carbon footprint of wholemeal bread production in Italy. J. Clean. Prod. 153, 309–319. https://doi.org/10.1016/j.jclepro.2017.03.111

Chrysoulakis, N., Lopes, M., San José, R., Grimmond, C.S.B., Jones, M.B., Magliulo, V., Klostermann, J.E.M., Synnefa, A., Mitraka, Z., Castro, E.A., González, A., Vogt, R., Vesala, T., Spano, D., Pigeon, G., Freer-Smith, P., Staszewski, T., Hodges, N., Mills, G., Cartalis, C., 2013. Sustainable urban metabolism as a link between bio-physical sciences and urban planning: The BRIDGE project. Landsc. Urban Plan. 112, 100–117. https://doi.org/10.1016/j.landurbplan.2012.12.005

Inamdar, A.K., French, A., Hook, S., Vaughan, G., Luckett, W., 2008. Land surface temperature retrieval at high spatial and temporal resolutions over the southwestern United States. J. Geophys. Res. Atmos. 113. https://doi.org/10.1029/2007JD009048

IPCC, 2014. Climate Change 2014: Mitigation of Climate Change, Working Group III Contribution to the Fifth Assessment Report of the Intergovernmental Panel on Climate Change. https://doi.org/10.1017/CBO9781107415416

Irons, J.R., Dwyer, J.L., Barsi, J.A., 2012. The next Landsat satellite: The Landsat Data Continuity Mission. Remote Sens. Environ. 122, 11–21. https://doi.org/10.1016/j.rse.2011.08.026

Jianjun, J., Jie, Z., Hong'an, W., Li, A., Hailong, Z., Li, Z., Jun, X., 2005. Land cover changes in the rural-urban interaction of Xi'an region using Landsat TM/ETM data. J. Geogr. Sci. 15, 423–430. https://doi.org/10.1007/BF02892149

Jimenez-Munoz, J.-C., Sobrino, J.A., 2008. Split-Window Coefficients for Land Surface Temperature Retrieval From Low-Resolution Thermal Infrared Sensors. IEEE Geosci. Remote Sens. Lett. 5, 806–809. https://doi.org/10.1109/LGRS.2008.2001636

Jimenez-Munoz, J.C., Cristobal, J., Sobrino, J.A., Sòria, G., Ninyerola, M., Pons, X., 2009. Revision of the single-channel algorithm for land surface temperature retrieval from landsat thermal-infrared data. IEEE Trans. Geosci. Remote Sens. 47, 339–349. https://doi.org/10.1109/TGRS.2008.2007125

Jiménez-Muñoz, J.C., Sobrino, J.A., Skokovi´, D., Mattar, C., Cristóbal, J., 2014. Land surface temperature retrieval methods from Landsat-8 thermal infrared sensor data. Geosci. Remote Sens. Lett. IEEE 11, 1840–1843. https://doi.org/10.1109/LGRS.2014.2312032

Karimi, V., Karami, E., Keshavarz, M., 2018. Climate change and agriculture: Impacts and adaptive responses in Iran. J. Integr. Agric. 17, 1–15. https://doi.org/10.1016/S2095-3119(17)61794-5

Karnieli, A., Agam, N., Pinker, R.T., Anderson, M., Imhoff, M.L., Gutman, G.G., Panov, N., Goldberg, A., 2010. Use of NDVI and land surface temperature for drought assessment: Merits and limitations. J. Clim. 23, 618–633. https://doi.org/10.1175/2009JCLI2900.1

Kolářová, M., Tyšer, L., Soukup, J., 2015. Weed species diversity in the Czech Republic under different farming and site conditions. Acta Univ. Agric. Silvic. Mendelianae Brun. 63, 741–749. https://doi.org/10.11118/actaun201563030741

Krčílková, Janovská, V., 2016. Land Tenure as a Factor Underlying Agricultural Landscape Changes in Europe: A Review. Sci. Agric. Bohem. 47, 68–81. https://doi.org/10.1515/sab-2016-0011

Kustas, W., Anderson, M., 2009. Advances in thermal infrared remote sensing for land surface modeling. Agric. For. Meteorol. 149, 2071–2081. https://doi.org/10.1016/j.agrformet.2009.05.016

Landis, D.A., 2017. Designing agricultural landscapes for biodiversity-based ecosystem services. Basic Appl. Ecol. 18, 1–12. https://doi.org/10.1016/j.baae.2016.07.005

Li, W., Saphores, J.D.M., Gillespie, T.W., 2015. A comparison of the economic benefits of urban green spaces estimated with NDVI and with high-resolution land cover data. Landsc. Urban Plan. 133, 105–117. https://doi.org/10.1016/j.landurbplan.2014.09.013

López, S., Wright, C., Costanza, P., 2016. Environmental change in the equatorial Andes: Linking climate, land use, and land cover transformations. Remote Sens. Appl. Soc. Environ. https://doi.org/10.1016/j.rsase.2016.11.001

Loveland, T.R., Irons, J.R., 2016. Landsat 8: The plans, the reality, and the legacy. Remote Sens. Environ. 185, 1–6. https://doi.org/10.1016/j.rse.2016.07.033

LPIS, 2018. No Title [WWW Document]. L. Parcel Identif. Syst. URL http://eagri.cz/public/app/lpisext/lpis/verejny2/plpis/

Masiello, G., Serio, C., Venafra, S., Liuzzi, G., Göttsche, F., Trigo, I.F., Watts, P., 2015. Kalman filter physical retrieval of surface emissivity and temperature from SEVIRI infrared channels: A validation and intercomparison study. Atmos. Meas. Tech. 8, 2981–2997. https://doi.org/10.5194/amt-8-2981-2015

NASA, N.A. and S.A., 2018. Atmospheric Correction Parameter Calculator [WWW Document]. URL https://atmcorr.gsfc.nasa.gov/

Parastatidis, D., Mitraka, Z., Chrysoulakis, N., Abrams, M., 2017. Online global land surface temperature estimation from landsat. Remote Sens. 9, 1–16. https://doi.org/10.3390/rs9121208

Pašakarnis, G., Morley, D., Malienė, V., 2013. Rural development and challenges establishing sustainable land use in Eastern European countries. Land use policy 30, 703–710. https://doi.org/10.1016/j.landusepol.2012.05.011

Pimentel, D., Burgess, M., 2013. Maintaining sustainable and environmentally friendly fresh produce production in the context of climate change, Global Safety of Fresh Produce: A Handbook of Best Practice, Innovative Commercial Solutions and Case Studies. Woodhead Publishing Limited. https://doi.org/10.1533/9781782420279.2.133

Quattrochi, D.A., Luvall, J.C., 1999. Thermal infrared remote sensing for analysis of landscape ecological processes: methods and applications. Landsc. Ecol. 14, 577–598. https://doi.org/10.1023/A:1008168910634

Ramankutty, N., Evan, A.T., Monfreda, C., Foley, J.A., 2008. Farming the planet: 1. Geographic distribution of global agricultural lands in the year 2000. Global Biogeochem. Cycles 22. https://doi.org/10.1029/2007GB002952

Roy, D.P., Wulder, M.A., Loveland, T.R., C.E., W., Allen, R.G., Anderson, M.C., Helder, D., Irons, J.R., Johnson, D.M., Kennedy, R., Scambos, T.A., Schaaf, C.B., Schott, J.R., Sheng, Y., Vermote, E.F., Belward, A.S., Bindschadler, R., Cohen, W.B., Gao, F., Hipple, J.D., Hostert, P., Huntington, J., Justice, C.O., Kilic, A., Kovalskyy, V., Lee, Z.P., Lymburner, L., Masek, J.G., McCorkel, J., Shuai, Y., Trezza, R., Vogelmann, J., Wynne, R.H., Zhu, Z., 2014. Landsat-8: Science and product vision for terrestrial global change research. Remote Sens. Environ. 145, 154–172. https://doi.org/10.1016/j.rse.2014.02.001

Schowengerdt, R.A., 2007. Remote sensing : models, and methods for image processing. Burlington, Massachusetts Acad. 3, 1–44. https://doi.org/10.1016/B978-0-12-369407-2.50004-8

Sklenicka, P., Molnarova, K.J., Salek, M., Simova, P., Vlasak, J., Sekac, P., Janovska, V., 2015. Owner or tenant: Who adopts better soil conservation practices? Land use policy 47, 253–261. https://doi.org/10.1016/j.landusepol.2015.04.017

Sklenicka, P., Zouhar, J., Trpáková, I., Vlasák, J., 2017. Trends in land ownership fragmentation during the last 230 years in Czechia, and a projection of future developments. Land use policy 67, 640–651. https://doi.org/10.1016/j.landusepol.2017.06.030

Sobrino, J.A., Jiménez-Muñoz, J.C., Paolini, L., 2004. Land surface temperature retrieval from LANDSAT TM 5. Remote Sens. Environ. 90, 434–440. https://doi.org/10.1016/j.rse.2004.02.003

Srivastava, P.K., Majumdar, T.J., Bhattacharya, A.K., 2009. Surface temperature estimation in Singhbhum Shear Zone of India using Landsat-7 ETM+ thermal infrared data. Adv. Sp. Res. 43, 1563–1574. https://doi.org/10.1016/j.asr.2009.01.023

Stoate, C., Báldi, A., Beja, P., Boatman, N.D., Herzon, I., van Doorn, A., de Snoo, G.R., Rakosy, L., Ramwell, C., 2009. Ecological impacts of early 21st century agricultural change in Europe - A review. J. Environ. Manage. https://doi.org/10.1016/j.jenvman.2009.07.005

Tello, E., Galán, E., Sacristán, V., Cunfer, G., Guzmán, G.I., González de Molina, M., Krausmann, F., Gingrich, S., Padró, R., Marco, I., Moreno-Delgado, D., 2016. Opening the black box of energy throughputs in farm systems: A decomposition analysis between the energy returns to external inputs, internal biomass reuses and total inputs consumed (the Vallès County, Catalonia, c.1860 and 1999). Ecol. Econ. 121, 160–174. https://doi.org/10.1016/j.ecolecon.2015.11.012

Tittonell, P. a, 2013. Farming Systems Ecology. Towards ecological intensification of world agriculture, Inaugural lecture upon taking up the position of Chair in Farming Systems Ecology at Wageningen University.

Tuomisto, H.L., Hodge, I.D., Riordan, P., Macdonald, D.W., 2012. Does organic farming reduce environmental impacts? - A meta-analysis of European research. J. Environ. Manage. 112, 309–320. https://doi.org/10.1016/j.jenvman.2012.08.018

U.S. Department of Interior, 2013. Using the USGS Landsat 8 Product. U.S. Dep. Inter. 1.

U.S.G.S., 2017. Landsat 8: Frequently Asked Questions [WWW Document]. URL https://landsat.usgs.gov/frequently-asked

U.S.G.S., 2015. USGS EarthExplorer. USGS Sci. a Chang. world.

U.S.G.S., 2013. Landsat 8: Quality band [WWW Document]. URL https://landsat.usgs.gov/qualityband

USGS, U.S.G.S., 2015. Landsat — Earth Observation Satellites Landsat Missions : Imaging the Earth Since 1972. Fact Sheet 3081, 2016. https://doi.org/DOI:10.3133/fs20153081

Valor, E., Caselles, V., 1996. Mapping land surface emissivity from NDVI: Application to European, African, and South American areas. Remote Sens. Environ. 57, 167–184. https://doi.org/10.1016/0034-4257(96)00039-9

Verburg, P.H., van de Steeg, J., Veldkamp, A., Willemen, L., 2009. From land cover change to land function dynamics: A major challenge to improve land characterization. J. Environ. Manage. https://doi.org/10.1016/j.jenvman.2008.08.005

Wan, Z., 2014. New refinements and validation of the collection-6 MODIS land-surface temperature/emissivity product. Remote Sens. Environ. 140, 36–45. https://doi.org/10.1016/j.rse.2013.08.027

Weng, Q., Lu, D., Schubring, J., 2004. Estimation of land surface temperature-vegetation abundance relationship for urban heat island studies. Remote Sens. Environ. 89, 467–483. https://doi.org/10.1016/j.rse.2003.11.005

Wulder, M.A., White, J.C., Loveland, T.R., Woodcock, C.E., Belward, A.S., Cohen, W.B., Fosnight, E.A., Shaw, J., Masek, J.G., Roy, D.P., 2016. The global Landsat archive: Status, consolidation, and direction. Remote Sens. Environ. 185, 271–283. https://doi.org/10.1016/j.rse.2015.11.032

Wulder, M.A., White, J.C., Masek, J.G., Dwyer, J., Roy, D.P., 2011. Continuity of Landsat observations: Short term considerations. Remote Sens. Environ. 115, 747–751. https://doi.org/10.1016/j.rse.2010.11.002

Xu, W., Gu, S., Zhao, X.Q., Xiao, J., Tang, Y., Fang, J., Zhang, J., Jiang, S., 2011. High positive correlation between soil temperature and NDVI from 1982 to 2006 in alpine meadow of the Three-River Source Region on the Qinghai-Tibetan Plateau. Int. J. Appl. Earth Obs. Geoinf. 13, 528–535. https://doi.org/10.1016/j.jag.2011.02.001

Yami, M., Snyder, K.A., 2016. After All, Land Belongs to the State: Examining the Benefits of Land Registration for Smallholders in Ethiopia. L. Degrad. Dev. 27, 465–478. https://doi.org/10.1002/ldr.2371

Yu, X., Guo, X., Wu, Z., 2014. Land surface temperature retrieval from landsat 8 TIRS-comparison between radiative transfer equation-based method, split window algorithm and single channel method. Remote Sens. 6, 9829–9852. https://doi.org/10.3390/rs6109829

Zagata, L., 2010. How organic farmers view their own practice: Results from the Czech Republic. Agric. Human Values 27, 277–290. https://doi.org/10.1007/s10460-009-9230-9

Ženka, J., Slach, O., Krtička, L., Žufan, P., 2016. Determinants of microregional agricultural labour productivity - Evidence from Czechia. Appl. Geogr. 71, 83–94. https://doi.org/10.1016/j.apgeog.2016.04.004

9. Annexes

9.1 Parcel Pairing Script

```
clc
clear
t0 = clock();

% Dates of Measuring
%     1 2 3 4   5 6   7  8    9    10 11 12   13   14 15   16   17
18 19
UM =
[1,2,7,7.5,9,9.5,10,14.5,16.5,19,22,25.5,27.5,28,29.5,30.5,31.5,32,3
6];
TXT_INP = [ '01_JAN_2015.txt';
            '02_FEB_2015.txt';
            '03_JUL_2015.txt';
            '04_JUL_2015.txt';
            '05_SEP_2015.txt';
            '06_SEP_2015.txt';
            '07_OCT_2015.txt';
            '08_FEB_2016.txt';
            '09_APR_2016.txt';
            '10_AUG_2016.txt';
            '11_OCT_2016.txt';
            '12_JAN_2017.txt';
            '13_MAR_2017.txt';
            '14_APR_2017.txt';
            '15_MAY_2017.txt';
            '16_JUN_2017.txt';
            '17_JUL_2017.txt';
            '18_AUG_2017.txt';
            '19_DEC_2017.txt'];


%% MANUALLY GIVEN INPUT INFORMATION
% LIMITS
DIS_lim = 2000;         % DISTANCE limit [m]
ELE_lim = 100;          % ELEVATION limit [m]
ASP_lim = 60;           % ASPECT limit [°]
SLO_lim = 1;            % SLOPE limit [%]
ARE_lim = 30;           % AREA limit [%]

% degree of polynomical aproximation
np = 8;

% T_SD_lim is the largest allowed standard deviation of parcel
  temperature
% (Parcels with greater deviation will be discarded)
T_SD_lim = [ ];  % [°c]
% T_SD_per_skip is the percentage of parcels with the highest
  standard
% deviation that will be discarded
T_SD_per_skip = [ ];    % [%]
%% MAIN CALCULATION

disp('Calculation in progress ..')
```

```
% Redefining variables
limits = [DIS_lim, ELE_lim, ASP_lim, SLO_lim, ARE_lim];
T0 = 0;
T1 = 0;
dT_MV = 0;
dT_SD = 0;


% Calculation
for inp = 1:length(TXT_INP)

        clear A AA B D Di T1i T0i dTi

        %% DATA IMPORT FROM TXT
        % Reading data from TXT file
      AA = dlmread(TXT_INP(inp,:), '',1,0);% Matrix AA contains all
                                           records
        %AA = dlmread(TXT_INP(inp,:), '',[1,0,10000,9]);


        %% SELECTING parcels
        % Matrix A contains all parcels with Significant Deviatin of
        % temperatures
        % meeting the requirement of SD_lim

        if isempty(T_SD_lim)==0
            AA = sortrows(AA,10);
            nA = length(find(AA(:,10)<=T_SD_lim)); % nA = number of
                                                     all
                                                 % parcels in
                                                   matrix
            A = AA(1:nA,:);
            T_SD_per = round(10*(100-nA/length(AA(:,1))*100))/10;
            T_SD_max = T_SD_lim;
        elseif isempty(T_SD_per_skip)==0
            AA = sortrows(AA,10);
            nA = round((100-T_SD_per_skip)*length(AA(:,1))/100);
                              % nA = number of all parcels in
                                   matrix
            A = AA(1:nA,:);
            T_SD_max = round(10*A(nA,10))/10;
            T_SD_per = T_SD_per_skip;
        else
            A = AA;
            T_SD_max = 0;
            T_SD_per = 0;
        end

        %% PARCEL TYPE SORTING
        % Sorting parcels into 2 different matrixes A0/A1, regarding
           parcel
        % type 0/1, CONVENTIONAL/ORGANIC respectively.
        % Matrix A0 contains all CONVENTIONAL parcels (type 0)
        % Matrix A1 contains all ORGANIC parcels (type 1)
```

```
% Sorting
A = sortrows(A,8);
[nA,~] = size(A);  % nA = number of all parcels in matrix A
n1 = sum(A(:,8));  % n1 = number of ORGANIC parcels in
                        matrix A1
n0 = nA-n1;        % n0 = number of CONVENTIONAL parcels in
                        matrix A0
A0 = A(1:n0,:);    % A0 = matrix with all CONVENTIONAL
                        parcels
A1 = A(n0+1:nA,:); % A1 = matrix with all ORGANIC parcels


%% MAIN CALCULATION

% Redefining variables
nB = 0;            % nB = Computing the results in matrix B
B = zeros(nB,4);   % B = Matrix with final pairs
                   % [ID_parc_1, ID_parc_0, LST_parc_1,
                      LST_parc_0]

% Variables usage for monitoring Nnumber of ORGANIC parcels
   Skipped
% because of not meeting the requirements of:
nSD = 0;    % DISTANCE limit
nSO = 0;    % OTHER limits


for i=1:n1  % For all ORGANIC parcels do...
    % D_min = The smallest still found distance between the
    % compared parcels
    D_min = DIS_lim+1;
    % D = Distances between i-ORGANIC parcel and all
    % CONVENTIONAL parcels
    D = sqrt((A1(i,6)-A0(:,6)').^2 + (A1(i,7)-A0(:,7)').^2);
    % Di = Positinos of CON parcels that meets the
           requirements
    % of DISTANCE
    Di = find(D<=DIS_lim);

    % Searches for CONVENTIONAL parcels, with the smallest
      distance
    % from the just monitored ORGANIC parcel
    for j=1:length(Di)

        % In the case of parcel distance is still the
           smallest
        if D(Di(j))<D_min
            % Calculation of deviations of measured
              parameters
            dev_calc = abs(A1(i,2:5)-A0(Di(j),2:5));
            % dev_calc = Calculated deviations of monitored
            % parametres [ELE_lim, ASP_lim, SLO_lim,ARE_lim]
            dev_calc(4) = dev_calc(4)/A1(i,5)*100;

            % Comparison of the calculated deviations with
            % the limit values
            dev_dif = limits(2:5)-dev_calc;
```

```
                    % In the case that all deviations are less than
                       limits
                    if min(dev_dif)>=0
                        D_min = D(Di(j));
                        b =
[A1(i,1),A0(Di(j),1),A1(i,9),A0(Di(j),9)];
                    end
                end
            end

            % Numbers of skipped ORGANIC parcels
            if isempty(Di)==1
                nSD = nSD+1;
            else
                nSO = nSO+1;
            end

            % If a CONVENTIONAL parcel, meeting all the limits, has
            % been found, the values are saved into matrix B
            if D_min<=DIS_lim
                nB = nB+1;
                B(nB,:) = b;
            end

        end


        %% STATISTICS
        % Rounding of temperatures
        B(:,3:4) = round(10*B(:,3:4))/10;
        T1i = (B(:,3));     % Tempreatures of ORGANIC parcels
        T0i = (B(:,4));     % Tempreatures of CONVENTIONAL parcels
        % Temperature Diferences between ORGANIC and CONVENTIONAL
           parcels
        dTi = T1i-T0i;
        % Mean values of temperature
        T0(inp) = round(100*sum(T0i)/nB)/100;
        T1(inp) = round(100*sum(T1i)/nB)/100;
        % Mean value of temperature difference
        dT_MV(inp) = round(100*sum(dTi)/nB)/100;
        % Standart deviation of mean value temperature difference
        dT_SD(inp) = round(100*sqrt(sum((dTi-
                     dT_MV(inp)).^2)/(nB)))/100;
        [H,p] = ttest(dTi);
        Results(inp,:) = [inp,T_SD_per,T_SD_max,n1,nB,n1-
                          nB,nSD,nSO,H,p,
                          dT_MV(inp),dT_SD(inp)];

        disp([TXT_INP(inp,:), ' - DONE'])

end
```

```
%% DISPLAYING THE RESULTS
format shortG

% Used LIMITES
disp(' ')
disp(' Used LIMITES:')
disp('   DIS_lim[m]     ELE_lim[m]    ASP_lim[°]   SLO_lim[%]
ARE_lim[%]')
disp(limits)


disp(' ')
disp('--------------')
disp('  RESULTS:')
disp('--------------')
disp(' ')
disp('                                                    |    Number of
ORGANIC parcels   |   |    Skiped because    |       H      p-value
Mean value   Standar deviation')
disp('           ID       Unused [%]   T_SD_max [°c]   ALL
USED        SKIPED      DIST>lim     OTHER>lim
dT_MV [°c]  dT_SD [°c]')
disp(Results)



%% PLOTS
Months = [1 2 3 4 5 6 7 8 9 10 11 12 1 2 3 4 5 6 7 8 9 10 11 12 1 2
3 4 5
          6 7 8 9 10 11 12];

%% Plot with mean values of temperature differences between ORGANIC
% and CONVENTIONAL parcels
figure
hold on
title(' ')
xlabel('Months of year')
ylabel('Temperature difference dT [°c]')

% plot(UM,dT_MV,'g--o')
% plot(UM,dT_MV-dT_SD, 'r')
% plot(UM,dT_MV+dT_SD, 'r')
bar(UM,dT_MV,'g')

% Polynomial aproximation
p = polyfit(UM,dT_MV,np);
xp = linspace(1,36,500);
yp = polyval(p,xp);
plot(xp,yp,'m','LineWidth',2)

% Adding numbers of months to the plot
plot([0,36],[0,0],'Color',[0 0 0])
for i=1:36
    text(i,-0.1,num2str(Months(i)),'Color',[0 0 0])
end
```